



저작자표시-비영리-변경금지 2.0 대한민국

이용자는 아래의 조건을 따르는 경우에 한하여 자유롭게

- 이 저작물을 복제, 배포, 전송, 전시, 공연 및 방송할 수 있습니다.

다음과 같은 조건을 따라야 합니다:



저작자표시. 귀하는 원저작자를 표시하여야 합니다.



비영리. 귀하는 이 저작물을 영리 목적으로 이용할 수 없습니다.



변경금지. 귀하는 이 저작물을 개작, 변형 또는 가공할 수 없습니다.

- 귀하는, 이 저작물의 재이용이나 배포의 경우, 이 저작물에 적용된 이용허락조건을 명확하게 나타내어야 합니다.
- 저작권자로부터 별도의 허가를 받으면 이러한 조건들은 적용되지 않습니다.

저작권법에 따른 이용자의 권리는 위의 내용에 의하여 영향을 받지 않습니다.

이것은 [이용허락규약\(Legal Code\)](#)을 이해하기 쉽게 요약한 것입니다.

[Disclaimer](#)

A DISSERTATION FOR THE DEGREE OF DOCTOR OF PHILOSOPHY

**Synthesis and Properties of
Silicone-Acrylic Pressure-Sensitive Adhesives
For Low Surface Energy Substrates**

저표면 에너지 기재 접착용
실리콘-아크릴레이트 점착제의 합성 및 물성

Advisor : Hyun-Joong Kim

by

Dong-Hyuk Lim

PROGRAM IN ENVIRONMENTAL MATERIALS SCIENCE

GRADUATE SCHOOL

SEOUL NATIONAL UNIVERSITY

FEBRUARY, 2016

SEOUL NATIONAL UNIVERSITY
GRADUATE SCHOOL
PROGRAM IN ENVIRONMENTAL MATERIALS SCIENCE

WE HEREBY RECOMMEND THE THESIS BY

Dong-Hyuk Lim

ENTITLED

Synthesis and Properties of Silicone-Acrylic Pressure-Sensitive
Adhesives For Low Surface Energy Substrates

BE ACCEPTED IN FULFILLMENT OF THE REQUIREMENTS
FOR THE DEGREE OF DOCTOR OF PHILOSOPHY

DECEMBER, 2015

COMMITTEE ON FINAL EXAMINATION

Chairman

Prof. Jae Young Jho

Co-Chairman

Prof. Hyun-Joong Kim

Member

Dr. JaeHeung Lee

Member

Dr. Chulho Kim

Member

Dr. Seunghan Shin

Abstract

Synthesis and Properties of Silicone-Acrylic Pressure-Sensitive Adhesives for Low Surface Energy Substrate

Dong-Hyuk Lim

Program in Environmental Materials Science

Graduate School

Seoul National University

Recently IT industry shows IoT (Internet of Things) trends such as smart electronic devices, wearable devices such as smart band, mobile-based fusion technology such as convergence of mobile-based financial service development. IT device becomes more compact and slim device and needs to be low cost.

IoT IT device needs to be flexibility, slim, compact appearance. So many slim electric parts are assembled by physical bonds such as bolts or chemical bond such as adhesive (including pressure-sensitive adhesive). Silicone materials are good substrates that have good heat spread, flexibility, anti-thermal shock ability, so many wearable devices uses silicone material for the flexible substrate. But silicone has low surface energy and flexible surface, so many adhesive or pressure sensitive adhesive have a difficult to bond. So, although silicone adhesive or pressure sensitive adhesive is expensive, for the bond to

low surface energy material, the silicone adhesive or pressure sensitive adhesive is used. In particular, pressure sensitive adhesive using silicone has to use the expensive fluorine-release films, so silicone pressure sensitive adhesive used on a limited basis.

In some papers, modified acrylic PSAs can be applied for a bond to low surface energy materials such as silicone. Modified acrylic PSA has main acrylic backbone such as 2-EHA (2-ethylhexyl acrylate), BA (butyl acrylate), AA (acrylic acid) with some low molecular functional additives such as PDMS crosslinking, fluorinated coupling agent or silicone modified branch structure.

In this study, modified acrylic PSA was synthesized by solution polymerization using PDMS-based macroinitiator (MAI, macro azo-based initiator). The MAI-acrylic PSAs used in this study were acrylic copolymers with different compositions. The model copolymers (poly-MAI-2EHA-IBA-AA copolymer) were synthesized by radical solution polymerization in a semi-batch procedure at 80 °C/6 hrs in a solvent (EA, ethylene acetate). To monitor the synthesis of polymerization, FTIR, Gel fraction, GPC, PSA performances such as peel strength, probe tack, shear adhesion were evaluated. For surface analysis, Raman spectroscopy, XPS was tested.

Based on this study, suitable process parameters and conditions are proposed for the synthesis of modified acrylic PSAs and optimized their adhesion performances on low surface energy substrates.

Keywords: pressure sensitive adhesive, low surface energy pressure sensitive adhesives, modified acrylic PSA, adhesion performance

Student Number : 2005-30361

Contents

Chapter 1

Introduction	12
---------------------------	----

Chapter 2

Experimental	17
2.1. Materials	18
2.2. Synthesis of modified acrylic PSAs	18
2.3. Formation of acrylate film	19
2.4. Adhesion performance	19
2.5. Instrumental analysis	20
2.6. Adhesion performance	38

Chapter 3

Results and Discussions	33
3.1. Synthesis and adhesion properties of MAI-acrylic PSAs with PDMS-based macro azoinitiator	34
3.2. Blending and adhesion properties of MAI-acrylic PSAs / Low Mw PSA / Polybutene(PB)	51
3.3. Adhesion properties and surface analysis of MAI-acrylate PSA / Low Mw PSA depending on dwell time	74

Chapter 4

Concluding Remarks 96

References 100

초록 110

List of Tables

Table 1. The properties of low molecular weight acrylic PSA.	28
Table 2. The properties of PB.	29
Table 3. The blend ratio of MAI-acrylic PSA and Low M_w acrylic PSA.	30
Table 4. Solution polymerization ratio of MAI-acrylate PSAs.	31
Table 5. The properties of contact angle ref. liquids.	32
Table 6. Molecular weight of MAI-PSAs by GPC.	50
Table 7. Viscoelastic properties related to PSA characteristics.	73
Table 8. Characteristics of some spectroscopic techniques suitable for studying polymeric materials.	93
Table 9. Contact angle photographs of MAI-acrylic PSA / LMW PSA.	94
Table 10. Atomic ratio of MAI-acrylic surface depending on dwell time.	95

List of Figures

Figure 1. Flexible devices and parts classification.	16
Figure 2. Chemical structure of monomers.	22
Figure 3. Chemical structure of PDMS-based macroinitiator.	23
Figure 4. Schematic diagram of probe tack process and its graph.	24
Figure 5. Schematic diagram of SAFT.	25
Figure 6. Contact angle of liquid/vapor interface.	26
Figure 7. Basic components of a XPS system.	27
Figure 8. Surface characteristics of silicon substrate and additional approach of silicone functionality to acrylic back bone.	40
Figure 9. Photograph of the mixtures of MAI and monomer, solvent.	41
Figure 10. IR spectrum of MAI.	42
Figure 11. IR spectrum of MAI-acrylic PSAs in specific range of 1500 to 750.	43
Figure 12. Molecular weight of MAI-acrylic PSAs by GPC.	44
Figure 13. Optical macroscopic photograph of MAI-acrylic PSAs.	45
Figure 14. UV-vis spectroscopy result of MAI-15.	46
Figure 15. Peel strength of MAI acrylic PSAs on SUS depending on MAI contents.	47
Figure 16. Probe tack of MAI acrylic PSAs depending on MAI contents. ...	48
Figure 17. SAFT(heat resistance) of MAI acrylic PSAs depending on MAI contents.	49
Figure 18. FTIR spectrum of MAI-15.	58
Figure 19. FTIR spectrum of low molecular weight acrylic PSA.	59
Figure 20. FTIR spectrum of polybutene(PB 1400).	60
Figure 21. Typical PSA performance as a function of molecular weight.	61

Figure 22. Peel strength of MAI-acrylic PSA onto SUS depending on low molecular weight acrylic PSAs content.	62
Figure 23. Peel strength of MAI-acrylic PSA onto Teflon depending on low molecular weight acrylic PSAs content.	63
Figure 24. Probe tack of MAI-acrylic PSA onto various substrates depending on low molecular weight acrylic PSAs content.	64
Figure 25. Peel strength of MAI-acrylic PSA blends onto SUS depending on PB M_w and PB content.	65
Figure 26. Peel strength of MAI-acrylic PSA blends onto Teflon depending on PB M_w and PB content.	66
Figure 27. Probe tack of MAI-acrylic PSA blends onto SUS depending on PB M_w and PB content.	67
Figure 28. Probe tack of MAI-acrylic PSA blends onto Cu depending on PB M_w and PB content.	68
Figure 29. Probe tack of MAI-acrylic PSA blends onto PE depending on PB M_w and PB content.	69
Figure 30. Probe tack of MAI-acrylic PSA blends onto PP depending on PB M_w and PB content.	70
Figure 31. Probe tack of MAI-acrylic PSA blends onto acrylic plate depending on PB M_w and PB content.	71
Figure 32. Probe tack of MAI-acrylic PSA blends onto Teflon depending on PB M_w and PB content.	72
Figure 33. Peel strength of MAI-acrylic PSA depending on dwell time on silicone substrate.	81
Figure 34. S-S curves of failure mode in MAI-acrylic PSA on silicone substrate.	82
Figure 35. Raman spectra of MAI.	83
Figure 36. Raman spectra of MAI-acrylic PSA.	84
Figure 37. Raman spectrometer of surface analysis in MAI-acrylic PSA. ...	85

Figure 38. Depth profile of MAI-acrylic PSA on 1 day dwell time.	86
Figure 39. Depth profile of MAI-acrylic PSA on 15 day dwell time.	87
Figure 40. Raman spectra of MAI-acrylic PSA depending on relative distance from interfacial layer.	88
Figure 41. Depth profile between MAI-acrylic PSA and silicone substrate on Raman spectra at 490 cm^{-1}	89
Figure 42. XPS results of MAI-acrylic PSA on 1 day dwell time.	90
Figure 43. XPS results of MAI-acrylic PSA on 15 day dwell time.	91
Figure 44. Si/Carbon atomic ratio of MAI-acrylic PSA depending on dwell time.	92

Chapter 1

Introduction

1. Introduction

IoT IT device needs to be flexible, slim, and compact. So many slim electric parts are bonded by physical bond such as bolts or chemical bond with adhesive (including pressure-sensitive adhesive). Silicone materials are good substrates that have good properties such as heat spreadability, flexibility, anti-thermal shock. Many wearable devices use silicone material as a flexible substrate. However, silicone substrates have low surface energy and flexible surface, and then pressure sensitive adhesive has a difficulty to bond it. Although the silicone adhesive or PSA is expensive, silicone adhesive or pressure sensitive adhesive should be used. In particular, pressure sensitive adhesive using silicone has to use the expensive fluorine-release films, so silicone pressure sensitive adhesive is used on a limited application (T. Ryhanen, *et al.*, 2010).

Flexibility can give many different properties to manufacturers and users. As a mechanical characteristic, it is conveniently classified in the three categories illustrated by Figure 1: (a) bendable or rollable, (b,c) permanently shaped, and (d) elastically stretchable. The tools for micro-fabrication have developed for flat substrates. Therefore, at present all manufacturing is done on a flat workpiece that is shaped only as late as possible in the process. This approach benefits from the tremendous technology base established by the planar integrated circuit and display industries.

Polymer substrates are highly flexible, can be inexpensive, and permit roll-to-roll processing. However, they are thermally and dimensionally less stable than glass substrates and are easily permeated by oxygen and water. A glass transition temperature (T_g) can be compatible with the device process

temperature. However, a high T_g alone is not sufficient. Dimensional stability and a low CTE are also important factors. Heating and cooling cycles shrink typical polymer films. They shrink less if prestabilized by prolonged annealing. Because the elastic modulus of polymer substrates is a factor of 10-50 lower than that of inorganic device materials, a small thermal mismatch stress can make the free-standing workpiece curve and cause misalignment during the overlay registration of the flattened piece. A large CTE mismatch coupled with a large temperature excursion during processing can break a device film. Polymer substrates with CTE below 20 ppm/°C are preferred as substrates for silicon-based device materials (Gleskova H. *et al.*, 1995, Gleskova H. *et al.*, 2002).

Acrylates and other suitable monomers are copolymerised to yield an acrylic copolymer of a specific composition. Crosslinking agents are usually added for improved cohesion. Acrylics can be synthesized in organic solvents. In this case, no further formulation is generally needed, although it is done from time to time in order to fine-tune their properties. Acrylics can also be synthesized in water but surfactants need to be added to make the polymer dispersible. The third group of acrylics is solvent free acrylic PSA. The composition of acrylate polymers that are inherently pressure-sensitive is a combination of soft (low T_g), hard (high T_g), and functional monomers in the polymer chain (Z.Czech, R. Milker, 2005).

As acrylic PSAs manufacturing was developed, some high-performance PSA becomes an alternative of some structural adhesive. This new adhesive, known as structural bonding tape, is an acrylic pressure-sensitive tape impregnated with an epoxy that cures under heat. This product can be cured in an oven at about 145°C for 20 min or hot bar cured. The composition of PSA polymers (before the curing process begins they are inherently

pressure-sensitive) is a combination of soft acrylate monomers with low T_g and hard epoxy monomers with high T_g in the polymer chain (Z. Czech *et al.*, 2004). The acrylic ester / epoxy resin pressure-sensitive thermosetting adhesive is an initially tacky and conformable thermosetting adhesive, which is obtained from a blend comprising epoxy resin or a mixture of about 20 ~ 60 wt. % epoxy resin and 0.5 ~ 10 wt. % of heat activatable hardener for the epoxy resins.

For making modified PSA which can be bonded onto low surface energy substrates, Silicone based modifiers are usually added. Modified acrylic PSA was synthesized by solution polymerization using PDMS-based macroinitiator (MAI, macro azo-based initiator). The MAI-acrylic PSAs used in this study were acrylic copolymers with different composition. The model copolymers (poly-MAI-2EHA-IBA-AA copolymer) were synthesized with radical solution polymerization with a semi-batch procedure at 80 °C / 6hrs in a solvent (EA, ethylene acetate). To monitor the synthesis of polymerization, FTIR, Gel fraction, GPC, PSA properties were evaluated. For surface analysis, Raman spectroscopy, XPS was tested .

The adhesive properties of modified PSAs can be controlled by MAI contents, monomers ratio, crosslinking density, M_w and dwell time. From surface analysis of MAI-arylic PSAs, mechanism of relationship between surface chemical composition and peel strength was studied.

Based on this study, suitable modified parameters and conditions are proposed for synthesis of modified acrylic PSAs, and optimization of adhesion properties onto low surface energy substrates can be achieved.

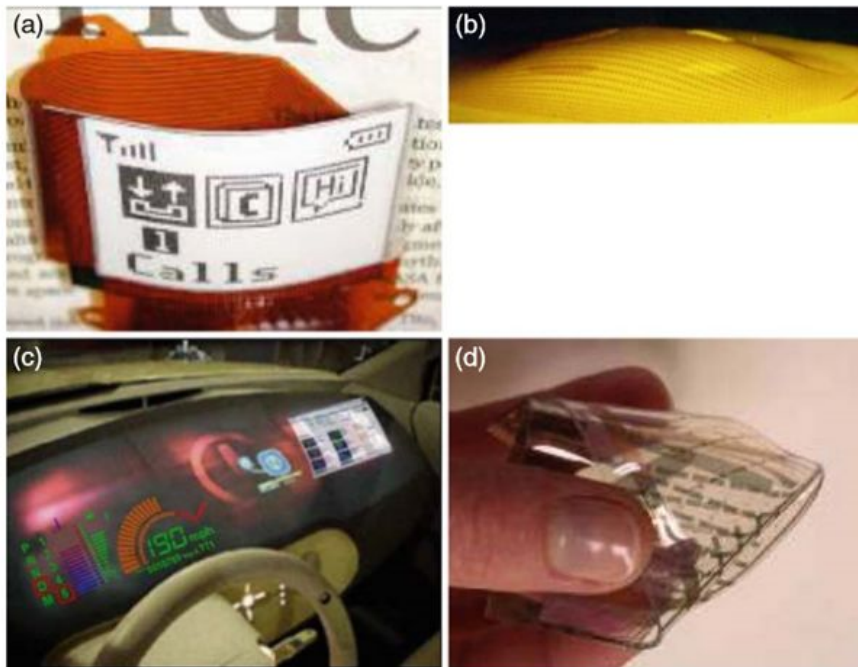


Figure 1. Flexible devices and parts classification (S. Wagner, *et al.* 2007)

(a) A bendable wristband display. (b) Silicon is lands on aspherically shaped foil substrate c) Concept for a conformably shaped digital dashboard (d) Stretchable interconnects on an elastomer.

Chapter 2

Experimental

2.1. Materials

The monomers, 2-ethylhexyl acrylate (2-EHA, from Junsei Chemical Co., Ltd), acrylic acid (AA, from Samchun Pure Chemical Co., Ltd) and Isobornyl acrylate (IBA, from Sigma Aldrich Co., Ltd) were all commercial grade available. The chemical structures of monomers were shown in Figure 2. The radical initiator is PDMS-based macroinitiator from Wako Pure Chemical Industries. The structure of the PDMS-based macroinitiator is shown in Figure 3. Low molecular weight adhesive is poly-2EHA-AA copolymer synthesized in radical polymerization (Table 1). Polybutene (PB) is commercial grade depending on molecular weight supplied from DEALIM Chemical Co., Ltd. (Table 2). The MAI-acrylic PSA/Low Mw PSA/PB blending ratio was shown in Table 3. silicone substrate is encapsulating material that is the elastic type to give the flexibility and the thermal stress absorption ability during reliability test.

2.2. Synthesis of modified acrylic PSAs

The MAI-acrylic PSAs used in this study were model statistical acrylic copolymers with a different composition which is listed in Table 4. The model copolymers (poly-MAI-2EHA-IBA-AA copolymer) were synthesized with radical solution polymerization in a batch procedure at 80 °C for 6hrs in a solvent (EA, ethylene acetate). The modified acrylic PSAs were synthesized depending on the MAI (VPS-1001) content from 5 to 20 phr. In MAI-0, thermal initiator of VPS-601 was used.

After polymerization, synthesized MAI-acrylic PSAs were evaluated by gel fraction. MAI-acrylic PSAs were coated onto Al foil. The samples were

weighted and immersed in toluene for 24 h at 50 °C, and then screened and dried at 80 °C to show a constant weight. The gel fraction of the samples was calculated using the following equation:

$$\text{Gel fraction (\%)} = W_t / W_0 \times 100, \quad (1)$$

Where W_0 and W_t are weight of samples before and after immersion, respectively. The gel content provides information on the degree of cross-linking (Wu *et al.*, 2010; Yang *et al.*, 2008).

2.3. Formation of acrylate film

MAI-acrylic PSAs were coated onto corona treated polyester film (PET, SK Chemicals, S. Korea) of 25 μm thickness using a No. 26 K-bar and kept at room temperature for 1 h, then dried in an oven at 100°C for 15min. These dried films were kept at 22°C \pm 2 and 60 \pm 5 % RH for 24 h before performing other tests.

2.4. Adhesion performance

- Probe tack

The probe tack was tested using a Texture Analyzer (Micro Stable Systems, TA-XT2i) with a 5mm diameter stainless steel cylinder probe. The measurements were carried out at a separation rate of 10mm/s under light pressure and a dwell time (1 sec.). In the debonding process, the probe tack results were obtained at the maximum debonding force (Figure 4).

- Peel strength

The stainless steel substrate was cleaned with acetone. Then, the PSA specimen was pressed onto the stainless steel substrate using 2 passes of a 2 kg rubber roller and stored at room temperature for over 12 hrs. The 180° peel strength of the PSA specimens was measured after being coated onto the polyester film. The cross head speed was 300 mm/min at room temperature. The average force in the debonding process was the peel strength.

- SAFT (Shear Adhesion Failure Temperature)

The shear adhesion failure temperature indicates the resistive ability under a constant shear load at an elevated temperature. The specimen was pressed onto a stainless steel substrate by a 2 kg rubber roller. The load attached to the specimen was 1 kg and the heating rate was 0.4°C/min. The SAFT results indicated the temperature at which the bonding failed (Figure 5).

2.5. Instrumental analysis

The FTIR spectra were obtained using a FTIR-6300 spectrometer (JASCO, UK) equipped with an attenuated total reflectance (ATR) accessory. The ATR crystal was zinc selenide (ZnSe) with a refractive index at 1000 cm⁻¹ of 2.4. It had a transmission range from 700 to 4,000 cm⁻¹. The resolution of the spectra recorded was 4 cm⁻¹ and the detector mode was TGS. All spectra were obtained with some correction, such as CO₂ reduction, H₂O reduction and a baseline correction.

The surface properties were measured using a contact angle test. Each sample was coated on glass using a 25 μm thickness applicator. The contact angle

was measured using a contact angle goniometer (SEO 300A contact angle measuring device, Surface & Electro-Optics Co., Republic of Korea). A single drop of distilled water, diiodomethane and ethylene glycol was placed on the surface of PSA, and detail characteristics of solution were shown in Table 5. The contact angle was observed after 5 sec on PSAs surface. The surface energy of PSAs was calculated by acid/base method. The bounce of the water drop on the coated PSAs surface was observed using a high speed camera (1000 frame/sec) in Figure 6.

Raman spectra radiation were taken for monitoring the surface change of PSA to depth direction using Horiba Jobin Yvon LabRam Aramis (Horiba, Japan) with Ar-ion laser beam at an exciting radiation wavelength of 785 nm. The Raman excitation beam size is about 1 μ m diameter. The assessed wavenumber range was 2000-100 cm^{-1} with a resolution of 1.3 cm^{-1} . The scanning were carried out 10 times from substrate to PSA at intervals of 1 μ m. 1 day dwelled PSA and 10 days dwelled PSA onto silicon substrate were compared with each other. The peaks at 490 cm^{-1} indicate Si-O-Si bond in macro azo initiator.

XPS was carried out to analyze the surface composition of the silicon-acrylate PSA using Flash 2000 (CE Elantech, USA) in Figure 7. Samples are prepared after peel test, and each samples are scanned from 93 eV to 113 eV binding energy in 1.00 eV and 0.1 eV steps to acquire higher resolution spectra of silicon 2p (S_{2p}), carbon 1s (C_{1s}), oxygen 1s (O_{1s}). The silicon to carbon ratio was determined from the peak areas using the standard atomic sensitivity factors (SF).

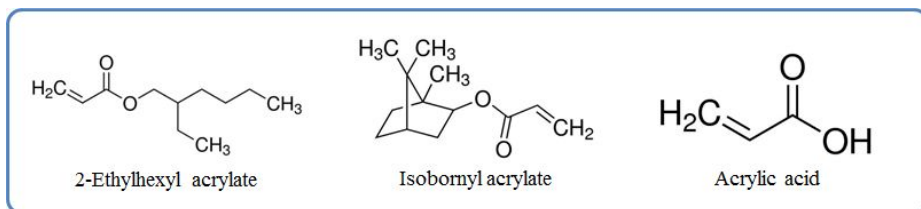


Figure 2. Chemical structure of monomers.

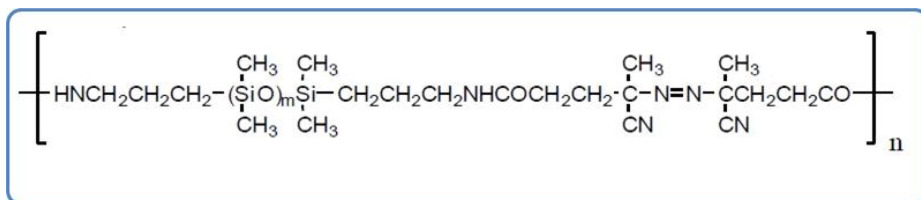


Figure 3. Chemical structure of PDMS-based macroinitiator

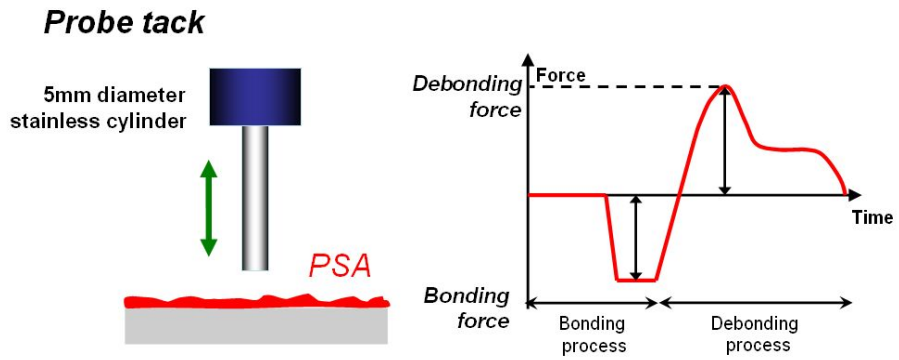


Figure 4. Schematic diagram of probe tack process and its graph

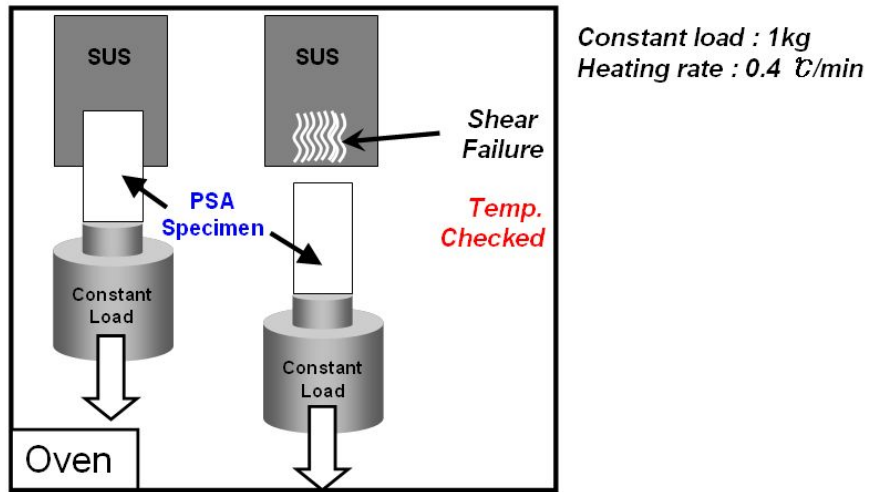
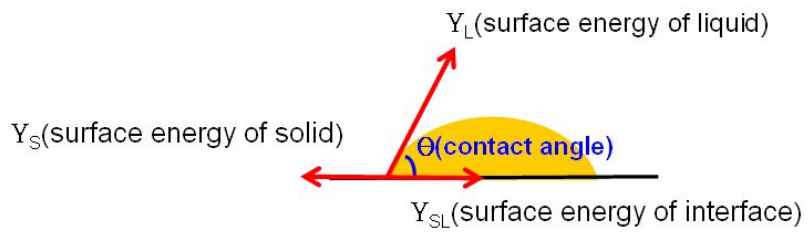


Figure 5. Schematic diagram of SAFT



Young equation : $Y_{SL} + Y_L \cos\theta$

Duprés equation : $W_A = Y_s + Y_L - Y_{SL}$

Young- Duprés equation : $W_A = Y_L(1 + \cos\theta)$

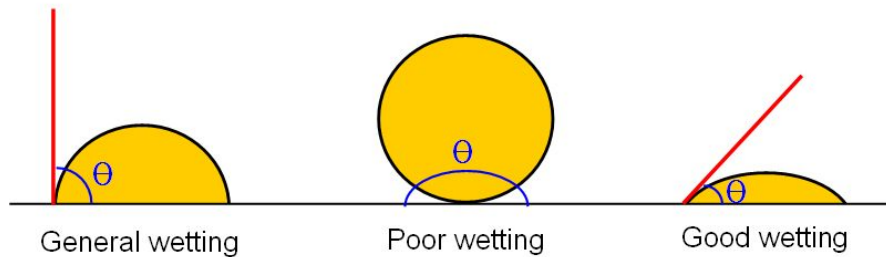
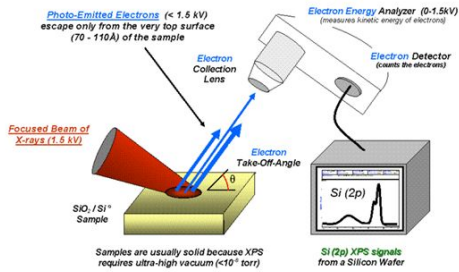


Figure 6. Contact angle of liquid/vapor interface

X-ray photoelectron spectroscopy (XPS, ESCA)



- ❖ elemental composition of the surface
- ❖ empirical formula of pure materials
- ❖ elements that contaminate a surface
- ❖ uniformity of elemental composition across the top the surface
- ❖ uniformity of elemental composition as a function of ion beam etching

Figure 7. Basic components of a XPS system.

Table 1. The properties of low molecular weight acrylic PSA

	SPEC.	Remark
Solid content (%)	40±1	105 °C, 2 hours
Viscosity (<i>cps</i>)	2,300	#5, 20 rpm, 23 °C
T_g (°C)	-31	DSC
M.W. (g/mol)	62,000	GPC
Solvent	Ethyl acetate	

Table 2. The properties of PB

Sample	M_n by GPC	Viscosity @40°C (<i>cps</i>)	Acid value (mg KOH/g)	T_g (°C)
PB-400	400	160	0.01	-30
PB-1400	1400	27,000	0.01	5

Table 3. The blend ratio of MAI-acrylic PSA and Low M_w acrylic PSA

Sample name	MAI-20	Low M_w acrylic PSA	X-500	Toluene
MAI20-LMW-0	100	0	0.22	10
MAI20-LMW-10	100	10	0.22	10
MAI20-LMW-20	100	20	0.22	10
MAI20-LMW-50	100	50	0.22	10

Table 4. Solution polymerization ratio of MAI-acrylate PSAs

VPS-1001^a: silicone based initiator

V-601^b: normal thermal azo based initiator

	MAI-0	MAI-5	MAI-10	MAI-15	MAI-20
2-EHA	75	75	75	75	75
AA	10	10	10	10	10
IBA	15	15	15	15	15
E.A.	150	150	150	150	150
VPS-1001 ^a	0	5	10	15	20
V-601 ^b	0.5				
S.C (%)	51	48	47	48	48

Table 5. The properties of contact angle ref. liquids.

Sample name	Tension	Dispersive	Polar	Acid	Base
Water	72.8	21.8	51	25.5	25.5
Ethyleneglycol	48.3	29	19.3	1.92	47
Diodomethane	50.8	50.8	0	0	0

Chapter 3

Results and Discussions

3. 1. Synthesis and adhesion Properties of MAI-acrylic PSAs with PDMS-based macro azoinitiator

Pressure-sensitive adhesives (PSAs) are unique in that they form a strong bond under relatively light pressure over short contact times. PSAs immediately grab onto a substrate (the material to which the PSA is applied) without the need for activation agents (e.g., heat, water, solvent, etc.). Among the various classes of adhesives, PSAs are possibly the most common adhesive found in consumer products. Self-adhesive tapes and labels of all kinds are ubiquitous in everyday life. Synthetic polymers based on acrylics, silicones, polyurethanes, or rubbers are preferred adhesive materials for use in commercial PSA systems because they display excellent performance. Acrylics may be optimized for the formulation of a PSA product by tuning certain preparation parameters. Acrylics are typically random copolymers of a long side-chain acrylic [n-butyl acrylate (BA) or 2-ethylhexyl acrylate (2-EHA)] with a low glass transition temperature (T_g), a short side-chain acrylic, such as methyl acrylate, which tunes T_g , and an acrylic acid (AA) that improves adhesion to polar substrates and optimizes the elongation properties of the material. PSAs can be applied as solventborne, waterborne (dispersions), or solvent-free systems (A. Kowalski, et al., 2013).

The surface free energy (SFE) is defined as the work needed beyond the magnitude of the forces holding the surfaces together to separate two surfaces in Figure 8. The SFE is given in units of energy per unit area, is often referred to as the surface tension, and having be expressed in units of dynes/cm. The SFE depends on the interfacial intermolecular forces and comprises the contributions from nonpolar (e.g., van der Waals) and polar (e.g., hydrogen bonding) components. The polar components can be further broken into

electron acceptor or electron donor components (or Lewis acid/ base components). Regions of a polar molecule will include a range of acceptor/donor component strengths, and in many regions, one component will be much more significant than the other (A. Kowalski, et al., 2013).

Acrylic PSA has larger surface energy than silicone substrate. Acrylic monomers are not sufficient to wet of silicone surface. So to bond to silicone substrate, it need to add some low surface energy components to acrylic back bone. Additional polymerizations of silicone component to acrylic back bone is below: using silicone based initiator, using silicone-acrylic monomer in backbone, using silicone-acrylic side branch chain. In this paper, modified acrylic PSA was synthesized by using silicone based initiator. Using silicone-acrylic monomer in the backbone and using silicone-acrylic side branch chain are critical. Silicone monomer has different surface tension with acrylic monomer. So a critical range of silicone monomer is needed (M. J. Zajackowski 2010).

Modified acrylic PSA in this study was synthesized by thermal polymerization using silicone based initiator. The polymerization process was monitored by FT-IR, GPC. To optimize adhesion properties, low M_w acrylic PSA and plasticizer are added in modified acrylic PSA. The adhesion properties were tested by peel strength and probe tack.

MAI is possible to dissolve in organic solvents and easily can introduce the the polydimethylsiloxane unit in the polymer chain. VPS-1001 as MAI has high molecular weight ($M_n=70,000\sim90,000$), and repeat unit M_n is about 10,000 .

Many researchers reported the superhydrophobicity and waterproof of general polymers can be increased by introducing PDMS structure (X. Zhang,

et al., 2007). For example, electrospun nonwoven mats composed of submicrometer diameter fibers of poly(styrene-*b*-dimethylsiloxane) block copolymers blended with PS-PDMS/PS. The wetting behavior of a solid surface is important for various commercial applications and depends strongly on both the surface energy or chemistry and the surface roughness. Other researcher approached that the synthesis of polymers has been the development of Atom Transfer Radical Polymerization (ATRP). This involves the use by an alkyl halide initiator in conjunction with a transition metal complex. The principle of ATRP is that the complex, for example, copper (I) bromide with bipyridyl, maintains an equilibrium between free polymer chains with active radical chain ends and complexed polymer chains. This ensures a low concentration of active radicals, minimising termination reactions. This allows 'living' conditions to be maintained during a radical polymerization so that materials with controlled molecular weight and polydispersity can be controlled. But, polymerization using PDMS based macro initiator is very simple approach to introduce PDMS structure to general polymer by radical thermal polymerization.

To check the miscibility of MAI, the mixture between MAI and monomers, solvents were made by physical stirring (ratio is 1:1). Figure 9 shows that MAI is miscible with 2-EHA, Toluene, EA, IBA. However, MAI is slightly miscible with AA. AA contains hydrophilic $-\text{COOH}$, so MAI and AA show a little miscibility in due to the difference of solubility parameter.

In Figure 10 is FTIR spectrum of MAI by ATR method. PDMS has characteristic peak related to Si-O, Si-O-Si, $\text{Si}-(\text{CH}_3)^2$, $\text{Si}-(\text{CH}_3)^3$, Si-C, CH_3 . The peak near 2200 cm^{-1} originated from CN bonding in MAI, and characteristic peaks in 1091, 1020 are related with Si-O and Si-O-Si.

Using MAI, poly-MAI-2EHA-IBA-AA copolymers were synthesized by solution polymerization according to the composition displayed in Table 4. The monomers such as 2-EHA, AA, IBA are static factors. MAI content is a controlled parameter in this polymerization. MAI's ten-hour half-life temperature is about 68 °C, but at about 70 °C, MAI shows a little efficiency, so polymerization temperature was increased to 80 °C. In a case of MAI-0, AIBN was used instead of MAI.

After polymerization, the functionality of MAI-acrylic PSAs were monitored by FTIR-ATR (Figure 11). FTIR spectrum shows acrylate related characteristic peaks such as 1717 cm^{-1} : the internal standard band of C = O stretching vibration of acrylate, 1695 cm^{-1} : carboxylic acid band, 1339 cm^{-1} : hydroxyl band, 1245 cm^{-1} : ester (-CO-O-) absorption band. In addition, it also shows 1091 cm^{-1} and 1020 cm^{-1} corresponding to Si-C and Si-O in PDMS structure. Si-O and Si-C peaks increased corresponding to MAI content. The modified acrylic PSA using MAI is well polymerized by radical reaction.

Figure 12 shows GPC results from polymerized MAI-acrylic PSAs. Depending on increasing MAI content, the number average molecular weight show gradually increasing from MAI content.

The increase of MAI content affects positively the polymerization conversion and molecular weight. The number average molecular weight shows a maximum at 15 phr of MAI in Table 6. The increase of MAI content has a beneficial effect on the molecular mass of synthesized PSA acrylics. In previous papers, radical polymerization, increase of initiator decreased M_n of PSA due to side reaction. The maximum molecular weight is 0.4 wt% AIBN content. For excess MAI content, PSA show low molecular weight in range

from 0.5~0.7 wt%.

MAI acrylic PSAs show a haze solution, so optical evaluation was tested in solution and dried film as shown in Figure 13 (magnification ratio : x2000). Reflective index of 2-EHA, IBA, AA is range of 1.48~1.49, but PDMS's reflective index is range of 1.40~1.43. The difference between PDMS and acrylate show a little immiscibility. The induced PDMS domain increase water repellence and decrease surface energy. Figure 14 is UV-visible spectroscopic results of MAI-acrylic PSA. In visible ray range, the loss of light is about under 1%.

In Figure 15, the peel strength of MAI-acrylic PSA shows that increasing MAI content effects higher peel strength. The MAI-0 is peel strength of acrylic PSA using AIBN. With comparing with acrylic PSA using AIBN, peel strength of MAI-acrylic PSA shows lower peel strength on SUS. Using MAI, the failure mode of fracture shows stick-slip. The stick-slip phenomenon is failure mode with cohesive and adhesive separation alternating in step with the oscillation of peel force. Rigidity of PSA effects this phenomenon. In previous papers, stick-slip was shown in high crosslinking density or high peeling speed and low temperature.

Probe tack results of MAI-acrylic PSA was shown in Figure 16. The MAI-0 is peel strength of acrylic PSA using AIBN. The probe tack of MAI-acrylic PSA is increasing depending on MAI content. Figure 25 shows S-S curve of probe tack. The probe tack is debonding force after 1 second with 100gf force press.

SAFT is an evaluation for cohesion or heat resistance of PSA. Figure 17 shows SAFT results of acrylic PSA using AIBN and MAI-acrylic PSAs.

Acrylic PSA using AIBN show about 60°C for failure. The MAI-acrylic PSA increases SAFT to 10 part of MAI, and then decreases SAFT to 20 part of MAI. MAI initiator increases heat resistance and cohesion of PSAs. due to high macromolecules.



Figure 8. Surface characteristics of silicon substrate and additional approach of silicone functionality to acrylic back bone

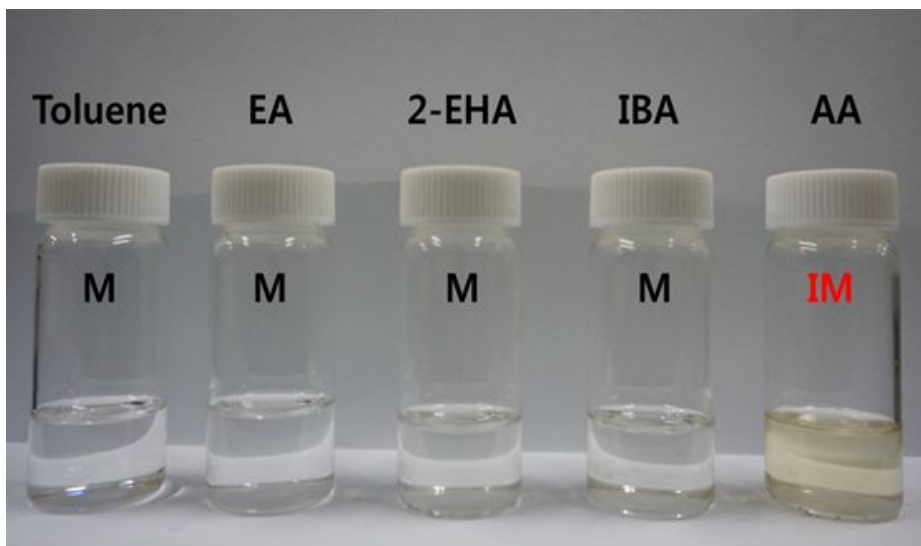


Figure 9. Photograph of the mixtures of MAI and monomer, solvent.
mixture ratio : (MAI: monomer or solvent = 1: 1), 2-EHA, Tol, EA show
good miscibility with MAI. AA show some reaction with VPS-1001

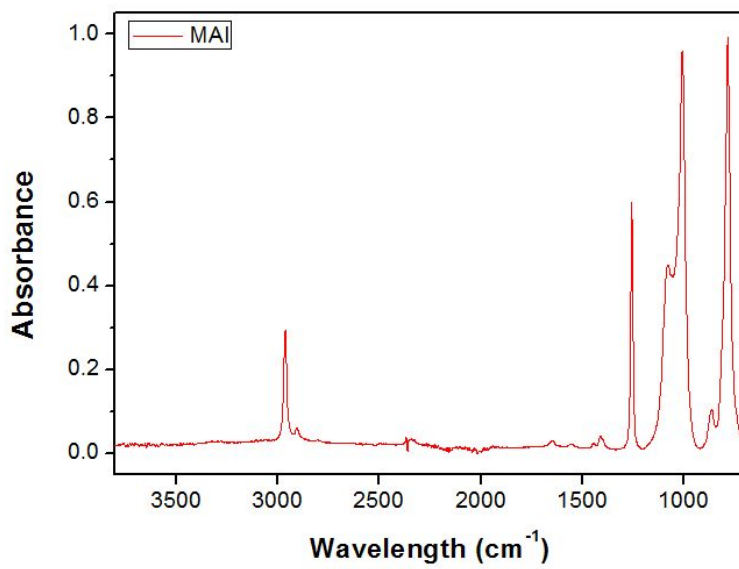


Figure 10. IR spectrum of MAI.

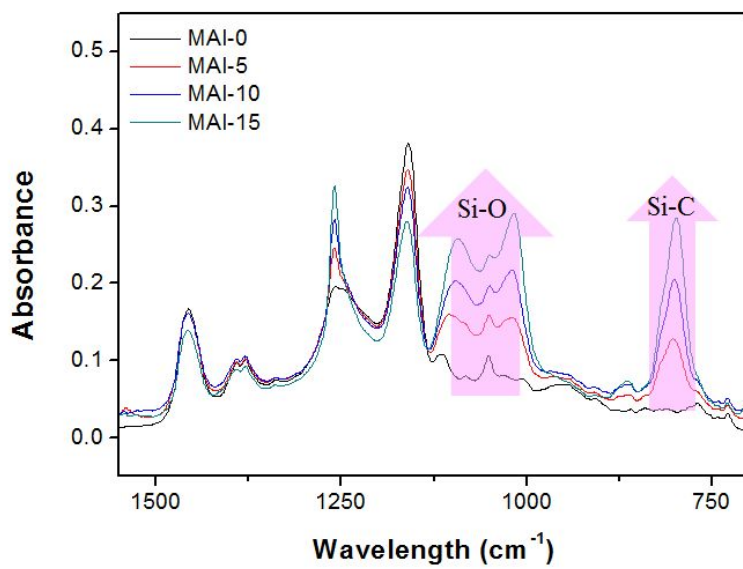


Figure 11. IR spectrum of MAI-acrylic PSAs in specific range of 1500 to 750.

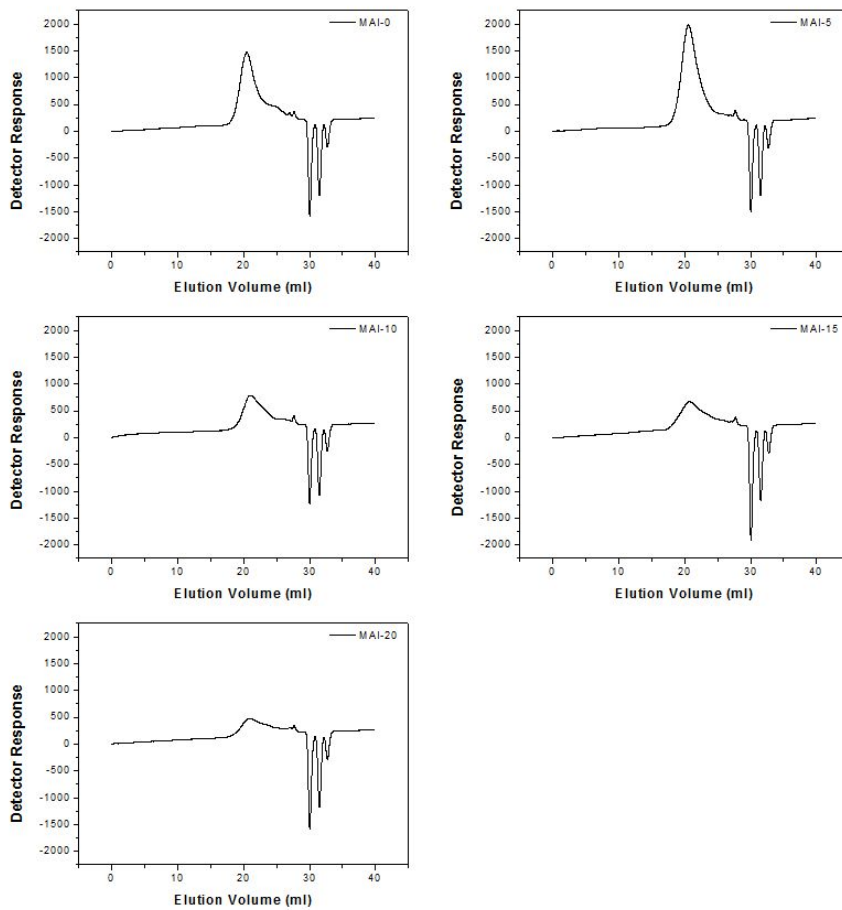


Figure 12. Molecular weight of MAI-acrylic PSAs by GPC

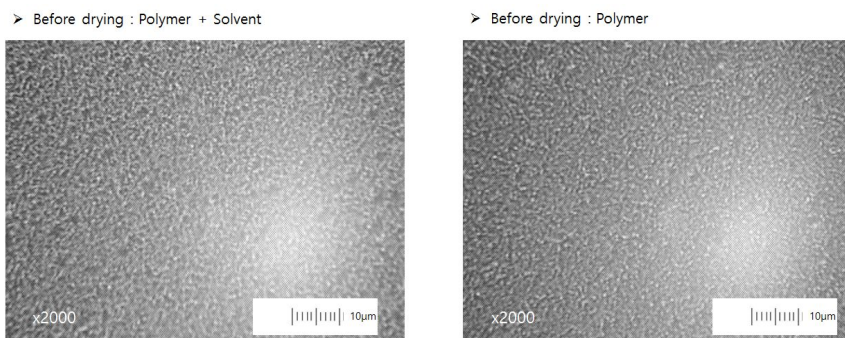


Figure 13. Optical macroscopic photograph of MAI-acrylic PSAs
upper : before drying / under : after drying

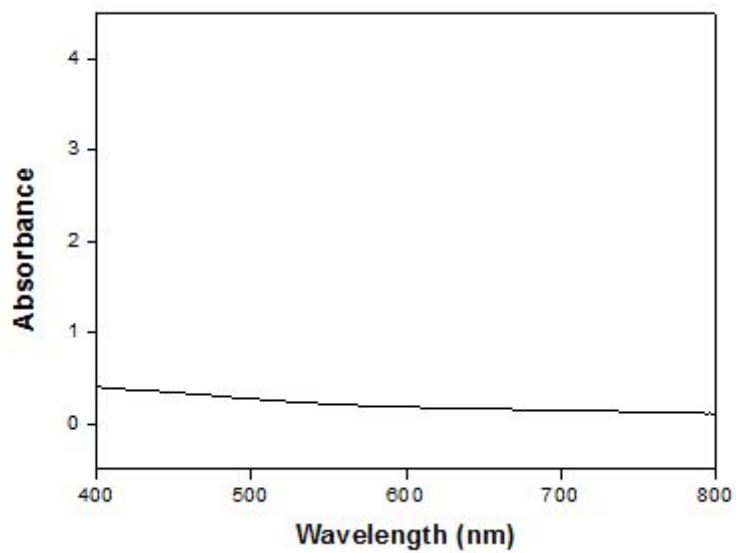


Figure 14. UV-vis spectroscopy result of MAI-15.

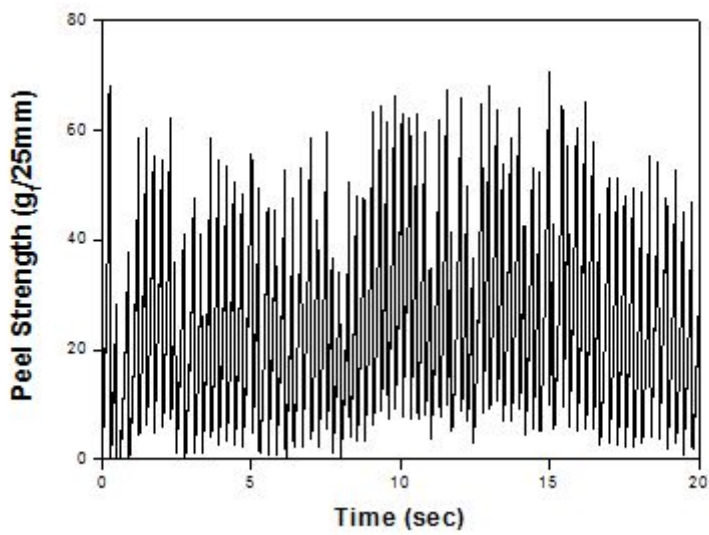
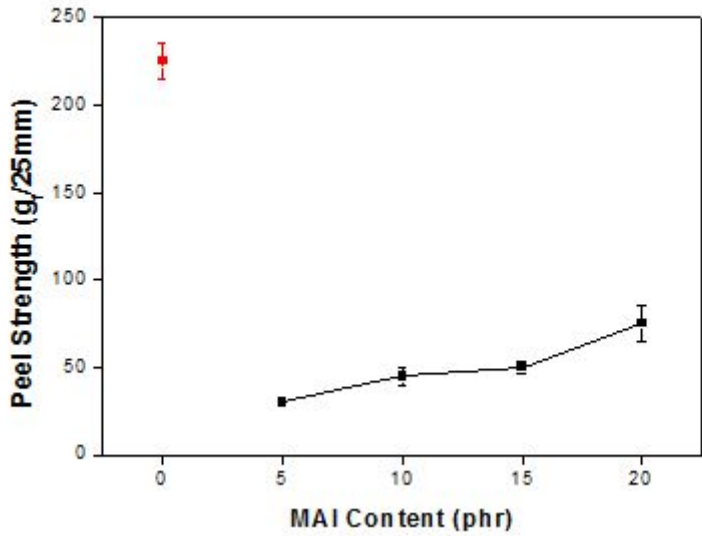


Figure 15. Peel strength of MAI acrylic PSAs on SUS depending on MAI contents(MAI 5~20 shows stick-slip failure).

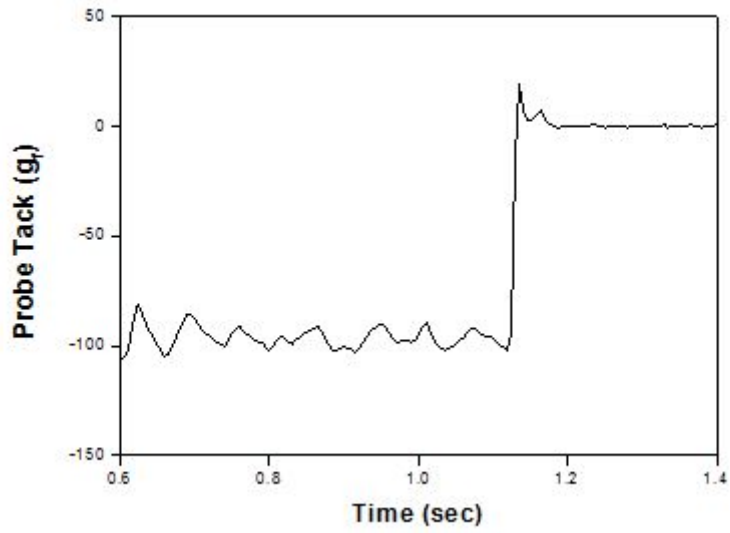
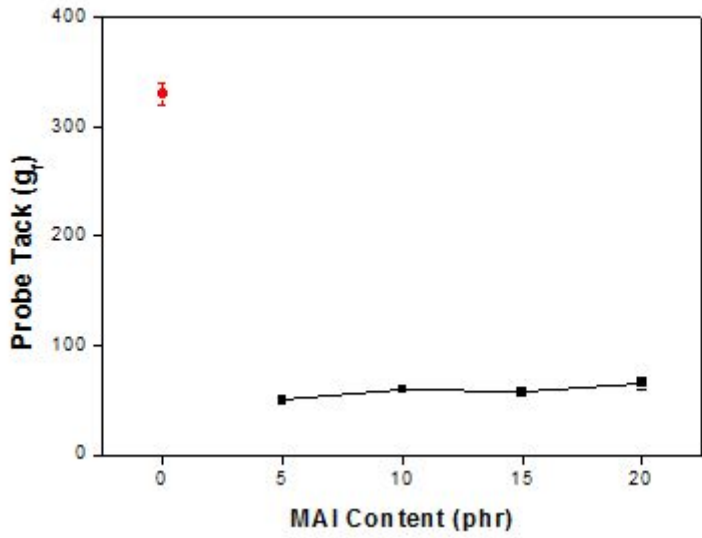


Figure 16. Probe tack of MAI acrylic PSAs depending on MAI contents.

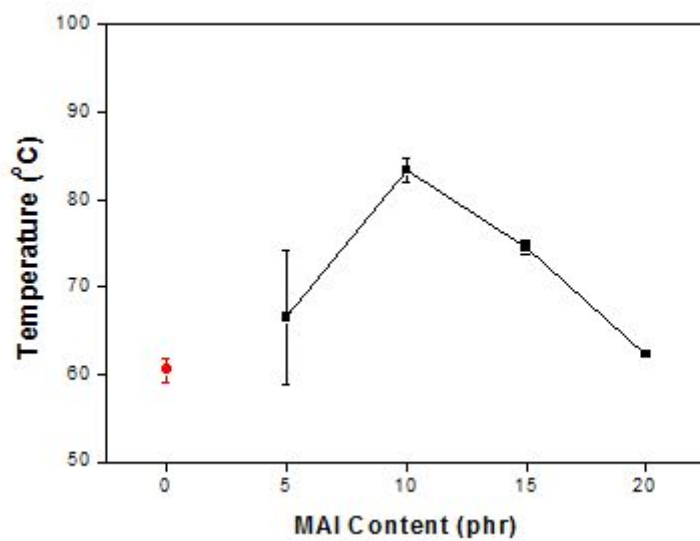


Figure 17. SAFT(heat resistance) of MAI acrylic PSAs depending on MAI contents.

Table 6. Molecular weight of MAI-PSAs by GPC

(0* : AIBN)

Sample	M_n (g/mol)	PDI
MAI-0	460,400	2.64
MAI-5	330,400	3.39
MAI-10	220,600	3.20
MAI-15	120,500	9.44
MAI-20	130,800	9.06

3.2. Blending and adhesion properties of MAI-acrylic PSAs / Low Mw PSA / Polybutene(PB)

Commercial use of pressure-sensitive adhesives (PSAs) covers broad range of label, medical and cosmetic products. The end-use properties of the PSAs will depend upon balance of peel strength and shear resistance, and the balance between these properties must be changed according to the specific end use of the PSA. The adhesion properties are characterized via measurements of two basic applicative properties: peel strength (the ability to resist removal by peeling), and shear resistance (the ability to resist flow when shear forces are applied). The adhesion properties are primarily influenced by the inherent properties of the polymer such as molecular weight. They have an influence on the polymer properties directly and as well as indirectly through their influence on the physical properties (e.g., glass transition temperature, T_g) (J. Asharaa, *et al.*, 2004).

Peel, tack and shear of PSAs strongly depend on the bulk rheological properties of PSAs. For a good PSA, the ratio of storage modulus at high frequencies to low frequencies should be high (E. P. Chang 2006). A higher loss tangent at higher frequencies than at low frequencies is also essential for a good adhesive and Chang reviewed the correlation of linear viscoelastic properties of pressure sensitive adhesive (PSAs) with industrial standard performances such as peel, tack and shear. The viscoelastic windows (VW) proposed by different workers were also compared for different types of pressure sensitive adhesives. One common viscoelastic criteria for a good performance PSA is the low bonding plateau modulus at the bonding frequency (low frequency) and high-energy dissipation at the debonding frequency (high frequency). Adhesion energy presented the PSA performance

as:

$$T = P_0BD$$

Where T is the adhesion performance. P_0 is the energy required to open up a unit area of PSA-metal interface in the absence of viscoelastic energy losses. B is characteristic of the bonding process and should remain constant for a given PSA test. D, strongly depending on separation speed of PSA test, is the viscoelastic loss component and is usually the dominant term in PSA tack. Bonding of adhesion has been found to correlate with the elastic moduli at low frequency [$G' (0.1 \text{ rad s}^{-1})$], and debonding has been shown to correlate with a ratio of the elastic moduli at both high and low frequency: $G' (100 \text{ rad s}^{-1}) / G' (0.1 \text{ rad s}^{-1})$. PSAs with $2 \times 10^5 \text{ dyne/cm}^2 < G' (\omega = 0.1) < 4 \times 10^5 \text{ dyne/cm}^2$ and $5 < G' (\omega = 100) / G' (\omega = 0.1) < 300$ would have an optimum combination of peel, tack and shear properties.

In rubber PSAs, Fujita *et al.* have investigated the effects of miscibility and viscoelasticity on shear creep resistance of natural rubber based PSAs. Hayashi *et al.* have investigated the relationship between the miscibility of acrylic copolymer/hydrogenated rosin systems and their performance. Kim *et al.* studied the influence of miscibility between the components in acrylic pressure-sensitive adhesives upon their peel strength P as a function of temperature has been studied. Kim *et al.* also investigated the effects of the properties of the substrates and tackifier on the characteristics of the Styrene-isoprene-styrene (SIS) based hot-melt pressure-sensitive adhesives (HMPSAs). Taghizadeh *et al.* studied the miscibility and tack of blends of poly (vinylpyrrolidone) (PVP)/acrylic pressure-sensitive adhesive (PSA). Blending of polymers provides an efficient way of developing new materials with tailored properties and thus has received much attention from both

academia and industry (Lee *et al.*, 2012).

In acrylic PSAs, inherent properties, such as copolymer composition and microstructure, molecular weight and molecular dispersity are among the most influential parameters affecting the PSA properties (J. Kajtnaa, *et al.*, 2008). An important problem regarding the use of the acrylic monomer system is the formation of a gel phase during the polymerization process. Recent studies show that the acrylate chain-growth kinetics is complicated by the intermolecular and intramolecular (backbiting) transfer to polymer and this process leads to formation of gel phase in the adhesive. The relative amounts of the sol and gel polymer phase as well as molar mass distribution of the sol fraction and the cross-linking density of the gel fraction are among the most important factors that influence the adhesive properties. The effect of different composition profiles of copolymer latex particles derived from 2-EHA/MA with similar MWDs on the adhesive properties were investigated by Laureau *et al.*. The effect of methyl methacrylate (MMA) on the tack in MMA/2-EHA copolymers for emulsion-based PSA was reported by Aymonier *et al.*. The possibility of tuning the adhesion properties through different holding tank temperatures, different types of chain transfer agents and the post-polymerization process were studied by Alarcia *et al.*.

Among the parameter, which are important for the successful blends of an appropriate PSA, is also monitoring of the molecular weight. In this study, low molecular weight acrylic PSA and polybutene were used to optimize an appropriate PSA performance in peel strength and probe tack.

FTIR spectrum of the low molecular acrylic PSA shows characteristic peak due to ester group stretching at 1736 cm^{-1} (A. Mata, *et al.*, 2005). Aliphatic C-H stretching due to $-\text{CH}_2$ and $-\text{CH}_3$ were observed at 2961, 2932 and 2862

cm^{-1} . Also, peaks due to aliphatic C-H bending due to $-\text{CH}_3$ was observed at 1462 cm^{-1} and C-H bending due to geminal dimethyl substitution was observed at 1381 cm^{-1} . The broad peak at 3452 cm^{-1} could be due to the traces of moisture that could be present during sample preparation for recording the spectrum (Figure 18, Figure 19).

In FTIR spectrum of PB, the bands at 905 and 925 cm^{-1} , corresponding to the CH_2 and CH_3 rocking vibrations, are known to be the characteristic of PB (Figure 20). The band at 1152 cm^{-1} derives from backbone CH_2 bending vibrations.

Acrylics as model polymers allow the exploration of the relative effects of surface and rheological behavior as a function of composition. Esters of acrylic acid with long alcohols may be used to form soft and tacky polymers of low glass transition temperature (T_g). The suitable monomers commonly reported in patent literature are alkyl acrylates and methacrylates of 4–17 carbon atoms (e.g. 2-ethylhexyl acrylate (2-EHA) which has a polymer T_g of $-70 \text{ }^\circ\text{C}$). To control the adhesive properties of PSA, the acrylic esters are almost always copolymerized with other monomers with generally higher T_g and/or proper functionality. An example of such a secondary monomer is acrylic acid (AA) with a polymer T_g of $106 \text{ }^\circ\text{C}$ and having carboxyl groups to provide cross-linking sites as well as providing a suspected improvement in adsorption properties. A typical acrylic PSA composition is 50–90% of a major monomer, 10–40% of a modifying monomer, and 2–20% of a monomer with desired functional groups. Composition plays an important role in the practical adhesive bonding characteristics of PSA (H. S. Tan, *et al.* 1999).

In Figure 21, molecular weight of acrylid PSA is very important factor to

optimize adhesion properties. Peel strength and shear strength can be variable with molecular weight. Acrylic PSAs observe an increase in peel adhesion and cohesive strength with increasing molecular weight to some maximum at which the cohesive strength exceeds the adhesive strength. Then subsequent increases in molecular weight result in higher cohesive strength at the expense of adhesion. One can see that the higher molecular weight polymer displays a broader range of cohesion/adhesion properties while the lower molecular weight material is much more limited (L. Christopher, *et al*, 2006).

Figure 22 show the peel strength of MAI-acrylic PSAs blends with low molecular weight PSA on SUS. Low molecular weight PSA effects on softness of PSA bulk properties so is increasing peel strength onto SUS. Carboxylic acid in acrylic PSA can be incorporated into the adhesive backbone during the polymerization. Acrylic acid is a high T_g monomer that, in addition to increasing cohesive strength, provides a polar moiety for bonding to polar substrates like metals and provide sites for crosslinking.

Decreasing molecular weight improves tack and peel strength while reducing heat resistance. For a given composition, the molecular weight distribution of the acrylic polymer must be optimized to obtain maximum performance. Higher T_g compositions require a relatively low molecular weight in order to maintain the ability to wet a surface. Softer compositions require higher molecular weight in order to display adequate cohesive strength.

Figure 23 show the peel strength of MAI-acrylic PSA blend onto Teflon. Polytetrafluoroethylene (PTFE) is a synthetic fluoropolymer of tetrafluoroethylene that has numerous applications. The best known brand name of PTFE-based formulas is Teflon by DuPont Co., which discovered the compound. Teflon is a fluorocarbon solid, as it is a high-molecular-weight

compound consisting wholly of carbon and fluorine. Teflon is hydrophobic: neither water nor water-containing substances wet Teflon, as fluorocarbons demonstrate mitigated London dispersion forces due to the high electronegativity of fluorine. Teflon is used as a non-stick coating for pans.. General PSA shows little peel strength onto Teflon. Addition of low molecule M_w PSA can increase peel strength depending on addition content. MAI-acrylic PSA but excess low molecule M_w PSA content is needed.

In Figure 24, the probe tack results of MAI-acrylic PSA blends with low molecular weight PSA. Low molecular weight PSA has molecular weight range from 10~50 phr. In range of 20~50 phr, probe tack results are not affected by low molecular weight PSAs. Low Mw PSA has no reactive functionality to low surface energy substrate, so Low Mw PSA is effect to adjust viscoelasticity of PSA not surface tension or wettability.

PB is lower molecular weight polymer, so it acts like plasticizer. Compounding these acrylic copolymers with plasticizer dramatically improves the balance of pressure sensitive adhesive properties while lowering viscoelasticity into a desirable range.

In Figure 25, the peel strength onto SUS increases with increasing PB content, but 40 phr content of PB is not good for peel strength. Increasing plasticizer content formulation from 0 to 10 phr caused a significant increase in peel strength and elongation of bulk PSA. PB 20~30 phr content formulation decreases in peel strength. Excess PB content caused a lower cohesion and a large elongation in steady lower peel strength.

In Figure 26, the peel strength onto Teflon is gradually increasing depending on increasing PB content. In contrast to SUS, all formulation show increasing

peel strength. Teflon has a little surface tension in comparison to SUS or metal. Peel strength is affected by mechanical properties of a PSA. In addition to the mechanical properties of a PSA, the composition must also provide the desired surface characteristics, one of these being surface energy. Surface energy determination for a PSA is both technologically relevant and practically challenging. It is difficult to determine the surface energies of soft polymers without provoking viscoelastic effects.

In Figure 27~32, the probe tack of blends with PB content were shown. In all probe materials, PB can be increasing probe tack. Especially PB 1400 show a good performance rather than PB400. This is shown that PB molecular weight is significant factor to optimized adhesion properties on low surface energy substrates such as plastics and silicone materials. Onto metal such as SUS and Cu, PB content in range of 10~20 phr shows maximum probe tack results. PB 1400 shows higher probe tack than PB 400. The higher molecular weight of PB can be good tacky properties on probe tack. On plastics such as PE, PP, Acrylic and Teflon, PB content in range of 30~40 phr shows good probe tack results. The good adhesion properties in plastics is more soft surface, so higher PB content samples show better probe tack results. In general, the wettability of organic surfaces is determined by the nature and packing of the surface atoms or exposed groups of atoms of the solid and is otherwise independent of the nature and arrangements of the underlying atoms and molecules. This exemplifies the extreme localization of the attractive field of force around covalent bonded atoms which are responsible for the adhesion of liquids to organic solids. The basic explanation is that the surface atoms in both classes of solids and liquids attract each other by highly localized attractive force fields such as the London dispersion forces, which decrease in intensity with the sixth power of distance (Shafrin and Zisman, 1960).

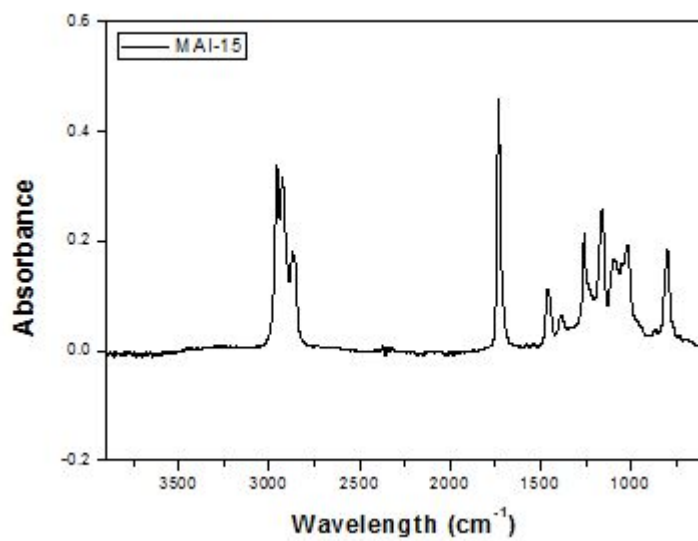


Figure 18. FTIR spectrum of MAI-15.

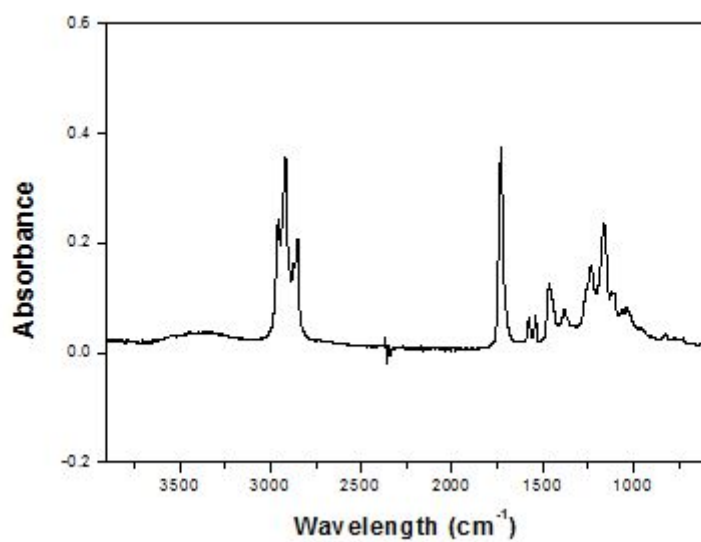


Figure 19. FTIR spectrum of low molecular weight acrylic PSA

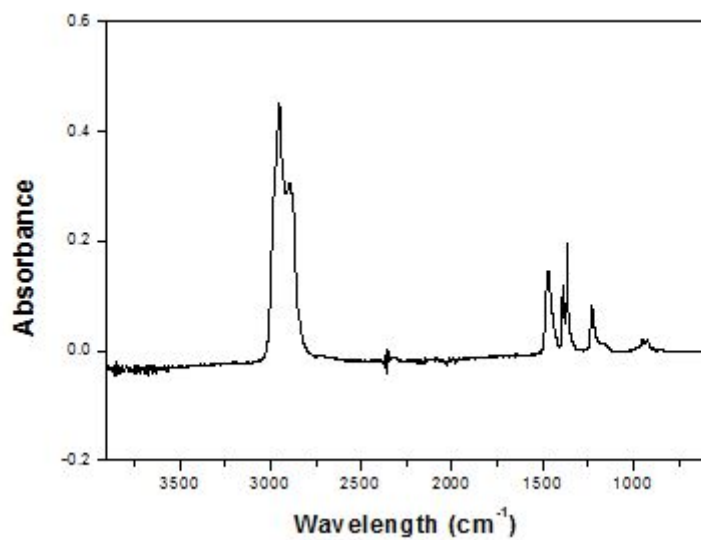


Figure 20. FTIR spectrum of polybutene(PB 1400)

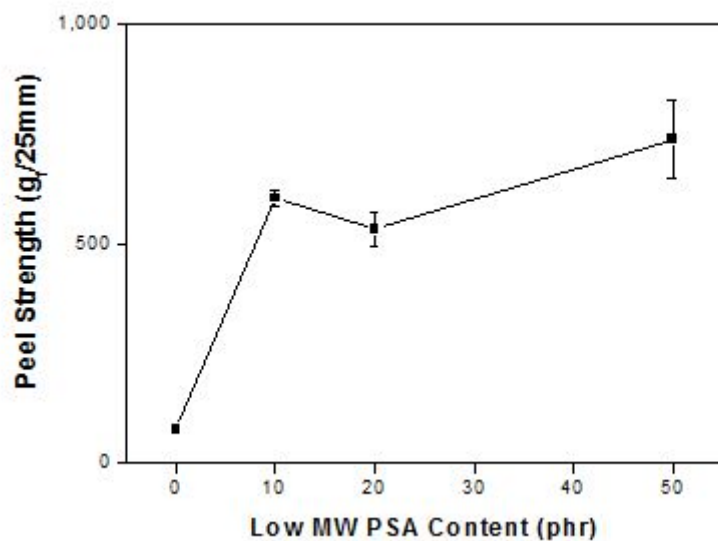


Figure 22. Peel strength of MAI-acrylic PSA onto SUS depending on low molecular weight acrylic PSAs content.

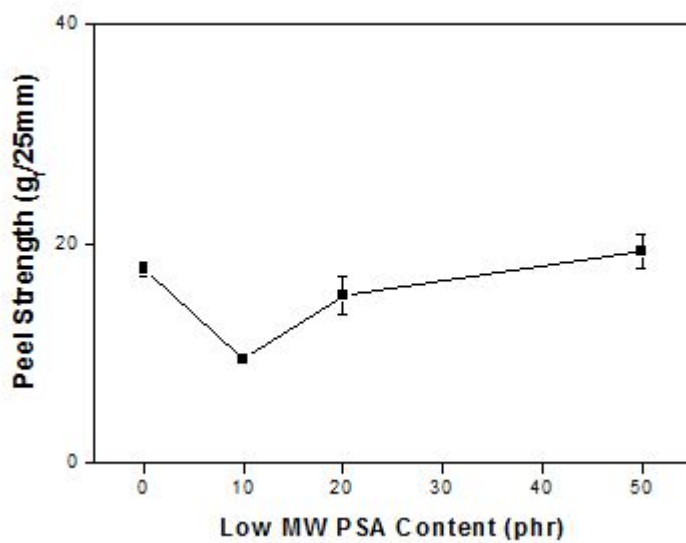


Figure 23. Peel strength of MAI-acrylic PSA onto Teflon depending on low molecular weight acrylic PSAs content.

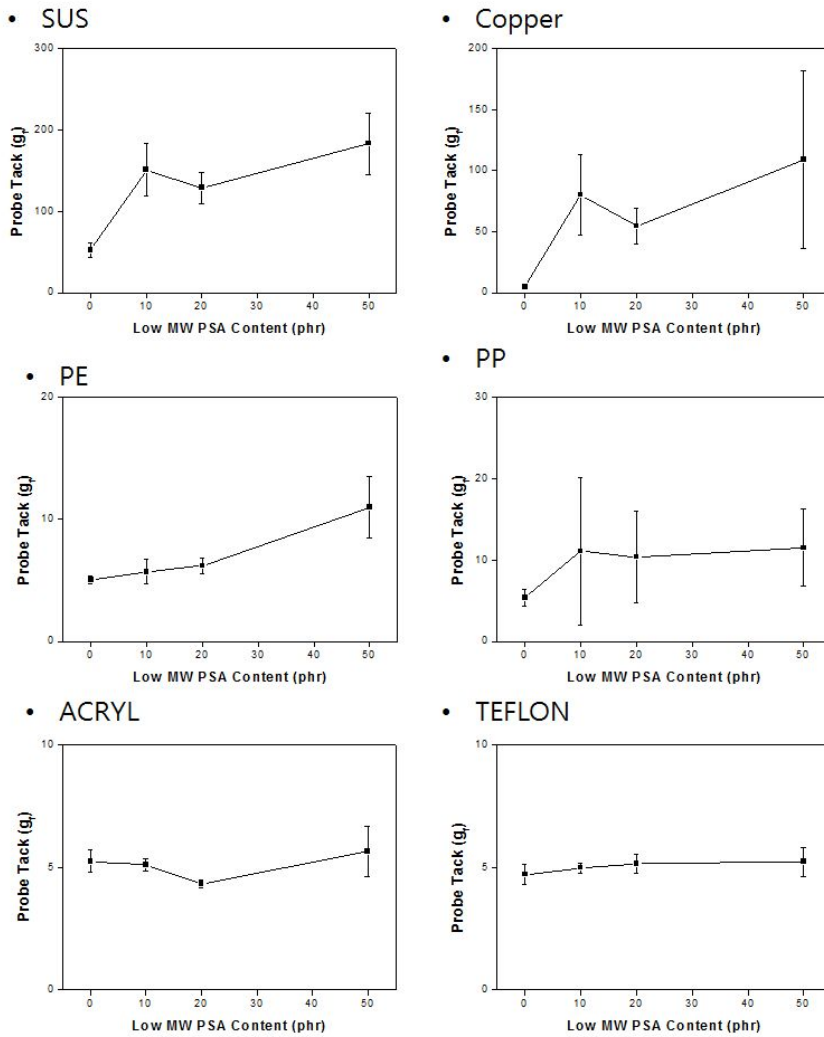


Figure 24. Probe tack of MAI-acrylic PSA onto various substrates depending on low molecular weight acrylic PSAs content.

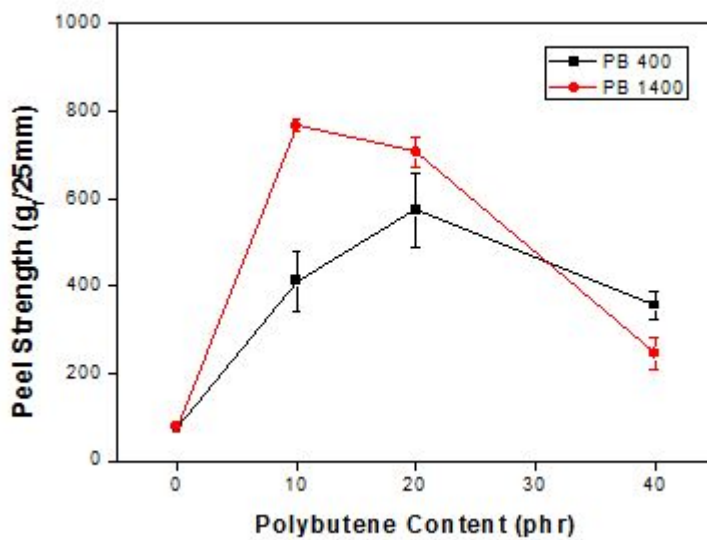


Figure 25. Peel strength of MAI-acrylic PSA blends onto SUS depending on PB M_w and PB content .

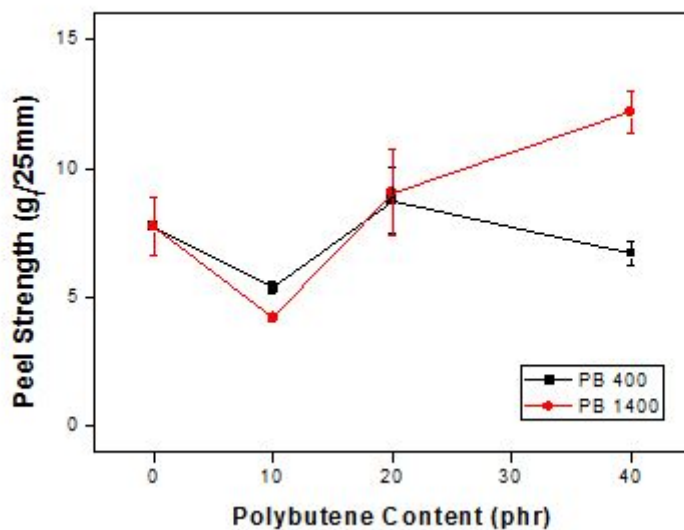


Figure 26. Peel strength of MAI-acrylic PSA blends onto Teflon depending on PB M_w and PB content .

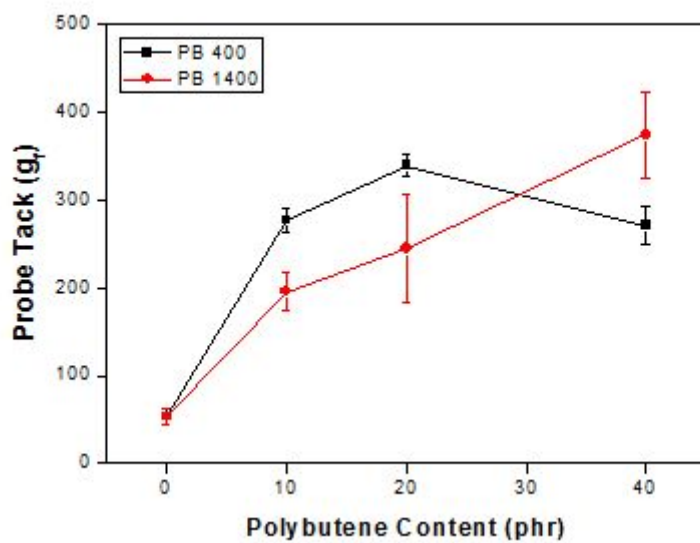


Figure 27. Probe tack of MAI-acrylic PSA blends onto SUS depending on PB M_w and PB content .

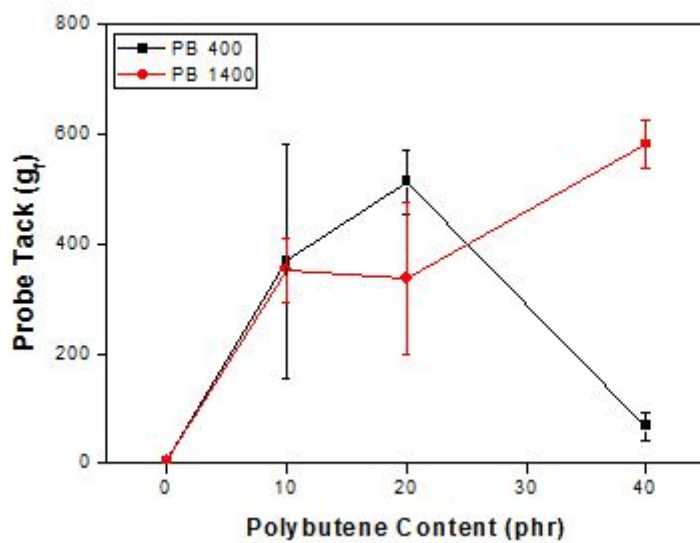


Figure 28. Probe tack of MAI-acrylic PSA blends onto Cu depending on PB M_w and PB content

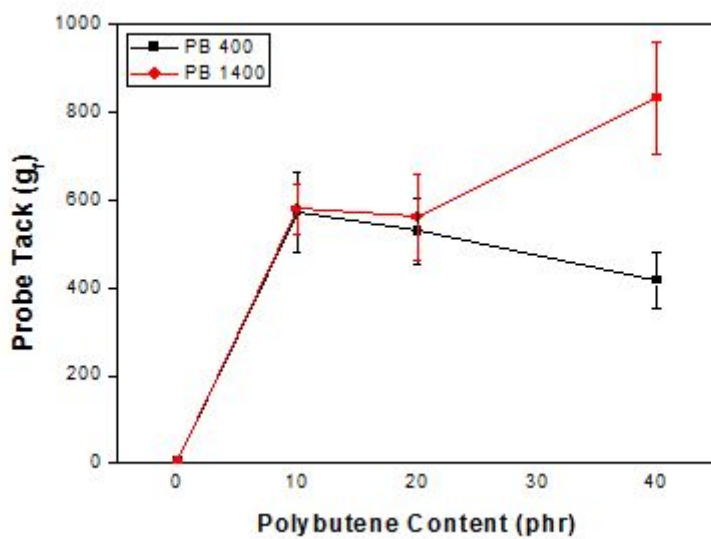


Figure 29. Probe tack of MAI-acrylic PSA blends onto PE depending on PB M_w and PB content

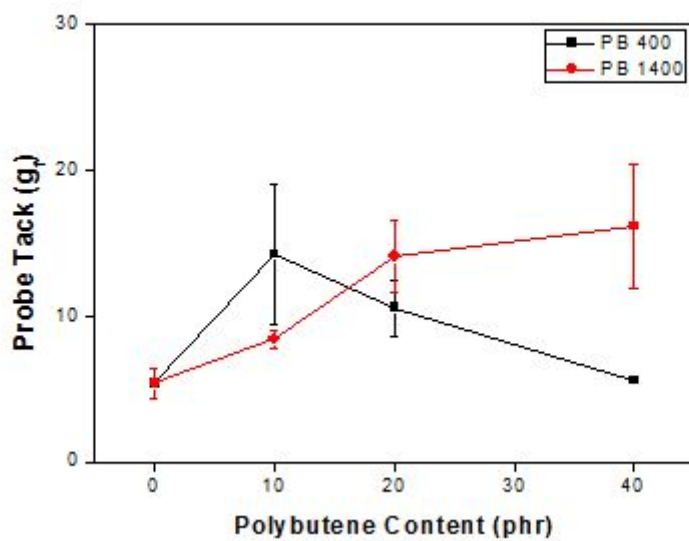


Figure 30. Probe tack of MAI-acrylic PSA blends onto PP depending on PB M_w and PB content

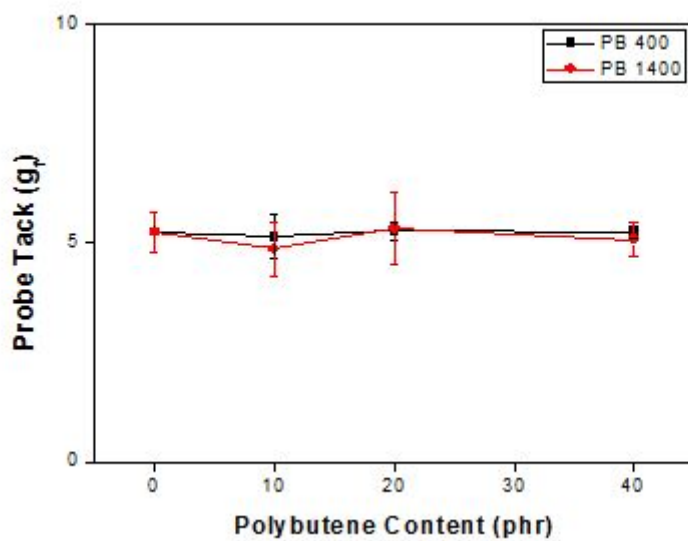


Figure 31. Probe tack of MAI-acrylic PSA blends onto acrylic plate depending on PB M_w and PB content

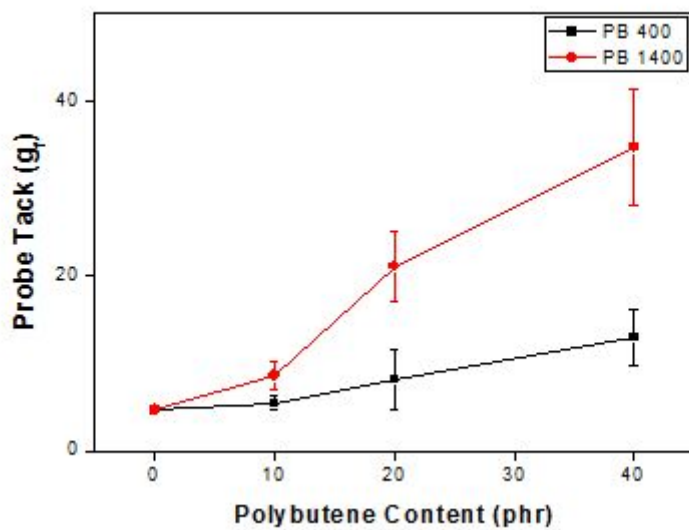


Figure 32. Probe tack of MAI-acrylic PSA blends onto Teflon depending on PB M_w and PB content

Table 7. Viscoelastic properties related to PSA characteristics (S. Sun).

Tack	- Low $\tan\delta$ peak and low G' - Low cross-links ($G'' > G'$) at ~ 1 Hz => High tack
Shear resistance	- High G' modulus at low frequencies < 0.1 Hz - High viscosity at low shear rates => High shear resistance
Peel strength	- High G'' at higher frequencies ($\sim > 100$ Hz) => High peel strength
Cohesive strength	- High G' and low $\tan\delta$ => High cohesive strength (bulk property)
Adhesive strength	- High G'' and high $\tan\delta$ => High adhesion strength with surface

3.3. Adhesion properties and surface analysis of MAI-acrylate PSA / Low Mw PSA depending on dwell time

Adhesion is the interatomic and intermolecular interaction at the interface of two surfaces. It is a multi-disciplinary topic which includes surface chemistry, physics, rheology, polymer chemistry, stress analysis, polymer physics and fracture analysis. Describing the mechanism of adhesion in simple terms is difficult due to the complexity and evolving understanding of the subject. The ultimate goal is to identify a single mechanism that explains adhesion phenomena. A range of adhesion mechanisms, based variously on diffusion, mechanical, molecular and chemical and thermodynamic adhesion phenomena, are currently the subject of debate in the literature (F. Awajaa, *et al.*, 2009).

Any consideration of adhesion mechanisms requires information about the physical and chemical properties of the adhering surfaces and the delamination surfaces in cases where adhesion has failed in use or as a result of mechanical testing. There are a number of surface characterization techniques utilized for investigating properties related to adhesion mechanisms and adhesion strength (B.D. Ratner, *et al.*, 1992). These include time-of-flight secondary ion mass spectrometry (ToF-SIMS), X-ray photoelectron spectroscopy (XPS), atomic force microscopy (AFM), secondary electron microscopy (SEM), attenuated total reflectance infrared spectroscopy (ATR-IR) and other microscopy techniques plus methods sensitive to surface energy such as optical contact angle analysis. There have been numerous studies which have looked at surface properties such as roughness, polarity, chemical composition and surface free energy to describe and explain adhesion phenomena at a surface or interface using the above

mentioned techniques.

Muppalla *et al.* reported that a general approach for the surface modification of varieties of poly(meth)acrylates and successful synthesis of new class of thermal plastic elastomers, composed of PDMS, acrylates and methacrylates (R. Muppalla, et al., 2012). They have demonstrated that the synthesized well-defined pentablock PMMA-PnBA copolymers and these copolymers show relatively high degree of phase separation, much superior oxidative stability and enhanced surface hydrophobicity.

Diethert *et al.* reported this investigation points out important parameters that influence the molecular composition of the near-surface region of adhesive films. Moreover, the influence of the installed composition profile on the adhesive properties is investigated. This knowledge about the possibility of a fine-tuning of the adhesive performance is beneficial for designing PSAs in special applications. In addition, it can be concluded that for punches with a small surface roughness, the main contribution to the mechanical performance comes from the surface-near region and with decreasing punch roughness it has to be expected that the surface component is of increasing importance(A. Diethert, *et al.*, 2010, Diethert, *et al.*, 2011) .

The MAI-acrylic PSAs were synthesized by solvent polymerization depending on MAI content in range of 0~15. MAI has urethane acrylate structure and PDMS structure, and can be miscible with acrylate resin and silicone resins. But on bond between semi-solid film (PSA film) and silicone film (substrate) needs a enough time (dwell time) due to molecular rearrangement. So peel strength of MAI-acrylic PSA was evaluated by dwell time in range of 0 ~ 15 days.

Figure 33 shows peel strength of MAI-acrylic PSA depending on MAI content. In case of MAI-0, peel strength is stable on dwell time. However As increasing MAI content from 5 to 15, peel strength of higher MAI content PSA show higher peel strength onto silicone substrate.

In 3 point of 10 days-MAI-10, 5 days-MAI-15, 5 days-MAI-15, failure mode of peel strength show interfacial failure which is debonding phenomenon between PSA and substrate. On other hands, all peel strength results except upper 3 points show stick-slip failure (Figure 34). The peeling failure mode undergoes from cohesive failure / interfacial failure between substrate and PSA / stick-slip / interfacial failure between backing material and PSA depending on peel rate or crosslinking density. The heterogeneous surface between PDMS phase of MAI and acrylic phase work on silicone substrate in initial bonding. This non-uniform surface caused heterogeneous peel phenomenon such as stick-slip. During dwell time, PDMS phase cause rearrangement between MAI-acrylic PSA surface and silicone substrate. Therefore stick-slip failure mode changes to interfacial failure between substrate and PSA surface (M.X. Xu, *et al.*, 1999).

The surface free energy (SFE) is defined as the work needed beyond the magnitude of the forces holding the surfaces together to separate two surfaces. The SFE is given in units of energy per unit area, is often referred to the surface tension, and may be expressed in units of dynes/cm (a surface tension of 1 dyne/cm or 1 mN/m is equivalent to a SFE of 1 mJ/m²). The SFE depends on the interfacial intermolecular forces and comprises the contributions from nonpolar (e.g., van der Waals) and polar (e.g., hydrogen bonding) components. The polar components can be further broken into electron acceptor or electron donor components (or Lewis acid/ base components). Regions of a polar molecule will include a range of

acceptor/donor component strengths, and in many regions, one component will be much more significant than the other. The SFE of a solid can be determined only indirectly by measuring the dynamic or static contact angles of various liquids, in combination with appropriate theoretical approaches (M. Schneemilch, *et al.*, 1998).

Contact angle of MAI-acrylic PSA / LMW PSA were evaluated using D.I. water, ethylene glycol, and diiodomethane. Three types of solution were stable in some angle onto acrylic PSA. The contact angle were shown in Table 8. Contact angle of acrylic PSA depending on MAI content was shown decreasing trend. PDMS molecular of acrylic PSA decrease contact angle in Table 8.

Experimental measurement of the contact angles enables the parameters such as polar (acid-base) and non-polar (dispersive) components to be calculated. The liquid thus acts as a sensitive probe by interacting chemically with functional groups at the surface. The total surface free energy (γ_s^{TOT}) of a given solid material (s) can be considered as composed of two parts: the Lifshitz-van der Waals (γ_s^{LW}) and the Lewis acid-base (γ_s^{SW}) components (Akovali *et al.*, 1998). The former represents the dispersion forces, dipole \pm dipole (Keesom) and induction (Debye), and the latter represents the short range H-bonding or acid-base interaction. This is written as the sum of the two components as equation.

$$(\gamma_s^{TOT}) = (\gamma_s^{LW}) + (\gamma_s^{SW})$$

The surface science of polymer materials has recently grown to a dynamic field, largely because of application in such areas as composite materials,

wetting, coatings, adhesion, friction, and biocompatibility. The synthesis of new polymer materials, resulting in desired polymer-surface structures and composition, has become more sophisticated and is driving the development of new spectroscopic probes and continuing evolution of more established methods.

A good example of how instrumentation development has led to better applications in polymer-surface science is to follow the growth of studies using x-ray photoelectron spectroscopy (XPS)—also called electron spectroscopy for chemical analysis (ESCA). ESCA is now routinely used to obtain surface composition of polymers, and to follow processing steps and degradation chemistry (Briggs *et al.*, 1998, Zhung, 1996). Advances in instrumentation have driven many of these more sophisticated applications in Table 9.

The MAI-acrylic PSA / LMW PSA blend is heterogenous material. For a better understanding of the influence of the inhomogeneities on the material properties, it is desirable to obtain information of the depth profile. To obtain directly the desired chemical and morphological information at high spatial resolution, infrared and Raman microscopies appear suitable techniques. Both Raman and infrared spectroscopy are prominent in the analysis of polymers, since they can yield a unique molecular fingerprint which contains information on the type and quantity of molecules prevalent, their structure (configuration and conformation), and the local environment they are in (i.e., amorphous or crystalline, oriented or unoriented). Compared to the extensively used infrared spectroscopy, Raman spectroscopy has a number of decisive disadvantages (i.e., the relative weakness of the Raman effect and the susceptibility of the technique to fluorescence). Generally, one applies

infrared spectroscopy to molecular finger-printing problems. However, Raman spectroscopy has a number of characteristics which make its use interesting for the chemical analysis at high spatial resolution. Most commonly, visible or near infrared laser light is used to excite the Raman scatter, and it is possible to use an ordinary optical light microscope as the excitation beam condenser and at the same time collect very efficiently the backscattered Raman for a subsequent spectral analysis. The main advantage in this context is the possibility to focus the probing laser beam to spot sizes of the order of 1 μm . A spatial resolution considerably higher is thus achievable with Raman as compared to infrared microscopy. Generally, it can be said that provided the sample under investigation is not fluorescent or light sensitive, the Raman spectroscopic analysis is relatively straightforward. No particular sample preparation is necessary, and sample alignment and focusing onto microscopic features in or on the sample are easy. Furthermore, the collection of the Raman scatter can be made confocal, improving lateral and depth spatial resolution significantly. By discriminating the extraneous light contributed by out-of-focus objects, the image contrast is dramatically improved. With a confocal microscope, it is possible to obtain sharp images of focal planes on the surface of or immersed in thick objects. Confocal Raman microscopy is now conveniently applied to point analysis and depth profiling of chemical and structural inhomogeneities, molecular orientation, and local stress. More recently, the efficient Raman analysis of whole areas of a sample has become a viable option by the development of Raman imaging. There are three principally different Raman imaging concepts based on conventional Raman spectroscopy (McCreery, 2005, Koenig, 1999).

Figure 35 features of Raman spectra of the MAI. Figure 35 show the 490 cm^{-1} of Raman spectra related to Si-O-Si of PDMS. Figure 36 features of Raman spectra in blends between MAI-acrylic PSA and LMW PSA. We assume that

490 cm^{-1} can be used by monitoring band for PDMS depth profile. The depth profiles of MAI-acrylic PSA / Low Mw PSA were evaluated by Raman microscopy in Figure 37 by $1\ \mu\text{m}$ scanning. The Raman spectras were shown in Figure 38 (1day) and Figure 39 (15 days). From Figure 38 and 39, monitoring of 490 cm^{-1} was shown in Figure 40. In interface between PSA and Si-substrate, the Si-O-Si band was slightly decreasing. However, the Si-O-Si band was increasing in $-1\mu\text{m}$ point. The total depth profile was shown in Figure 41. The interface between MAI-acrylic PSA and Si-substrate after 1day shows a discontinuous graph in the interface. After 15 days, the interface between MAI-acrylic PSA and Si-substrate show the decreasing discontinuity. The dwell time effects rearrangement of PDMS unit on MAI-acryli PSA due to good miscibility between MAI and Si-substrate.

To evaluate chemical composition of MAI-acrylic PSA's surface, the fracture surface of MAI-acrylic PSA with dwell time was evaluated by XPS. Figure 42 is the XPS result of MAI-acrylic PSA on 1 day dwell time, and Figure 43 is the XPS result of MAI-acrylic PSA on 15 days dwell time. The atomic ratio of MAI-acrylic surface depending on dwell time is shown in Table 10. From Figure 44 that shows Si/C atomic ration on dwell time, the dwell time is increasing Si/C atomic ratio in the fracture surface of MAI-acrylic PSA. The results of XPS shows the similar surface analysis result with Raman spectra.

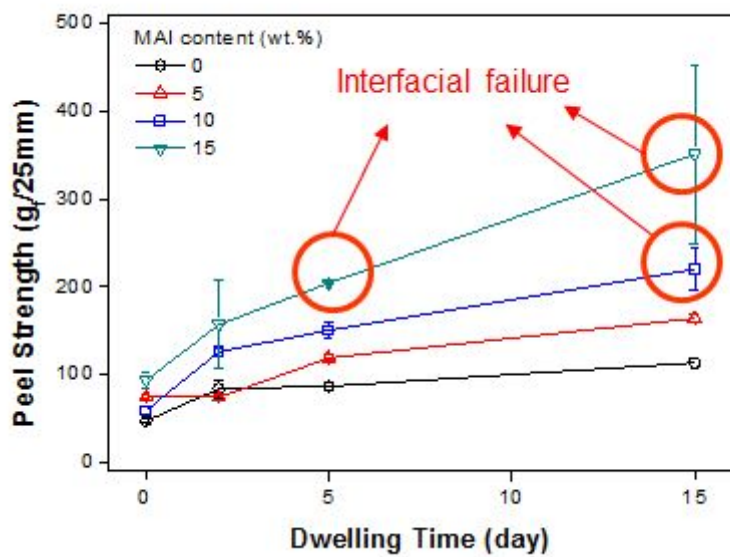
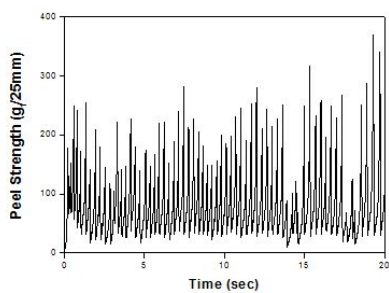


Figure 33. Peel strength of MAI-acrylic PSA depending on dwell time on silicone substrate.

✓ Stick Slip
(MAI_15wt.% 1h)



✓ Interfacial Failure
(MAI_15wt.% 15 days)

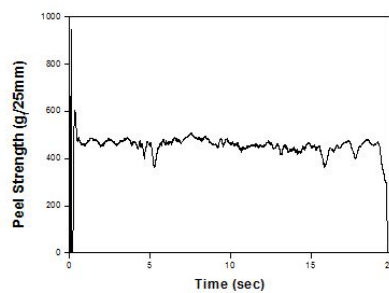


Figure 34. S-S curves of failure mode in MAI-acrylic PSA on silicone substrate.

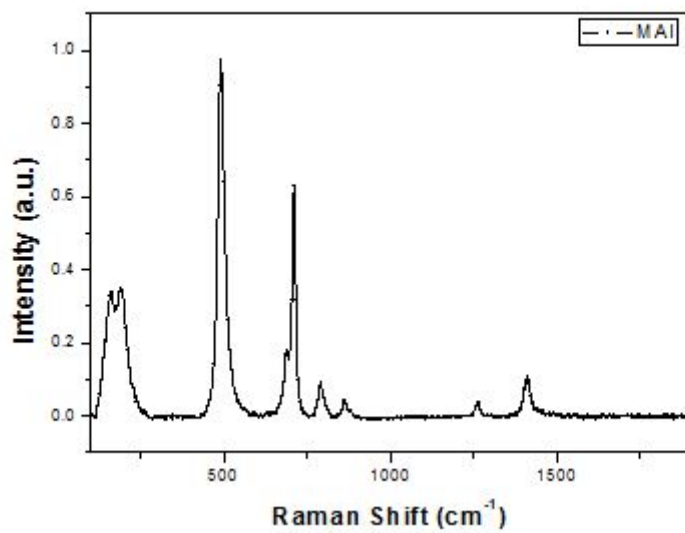


Figure 35. Raman spectra of MAI .

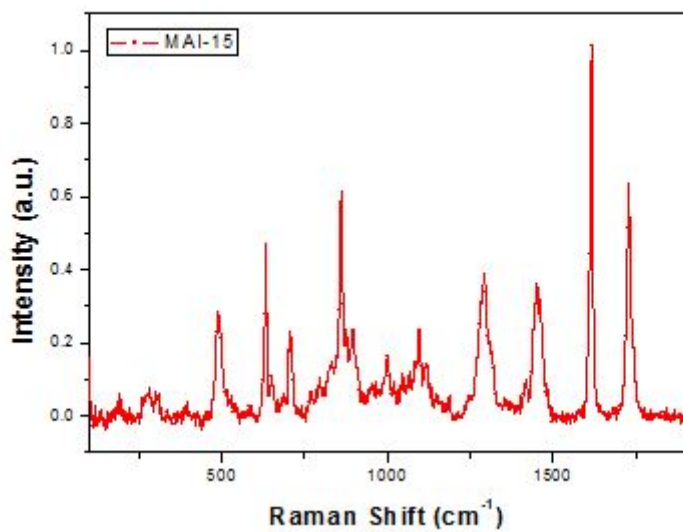


Figure 36. Raman spectra of MAI-acrylic PSA .

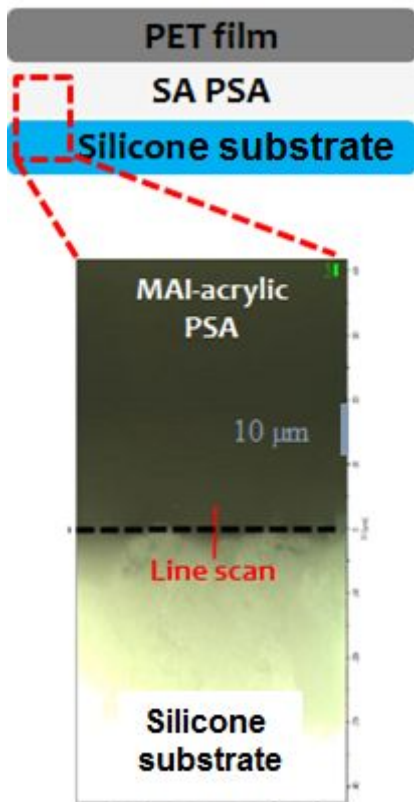


Figure 37. Raman spectrometer of surface analysis in MAI-acrylic PSA.

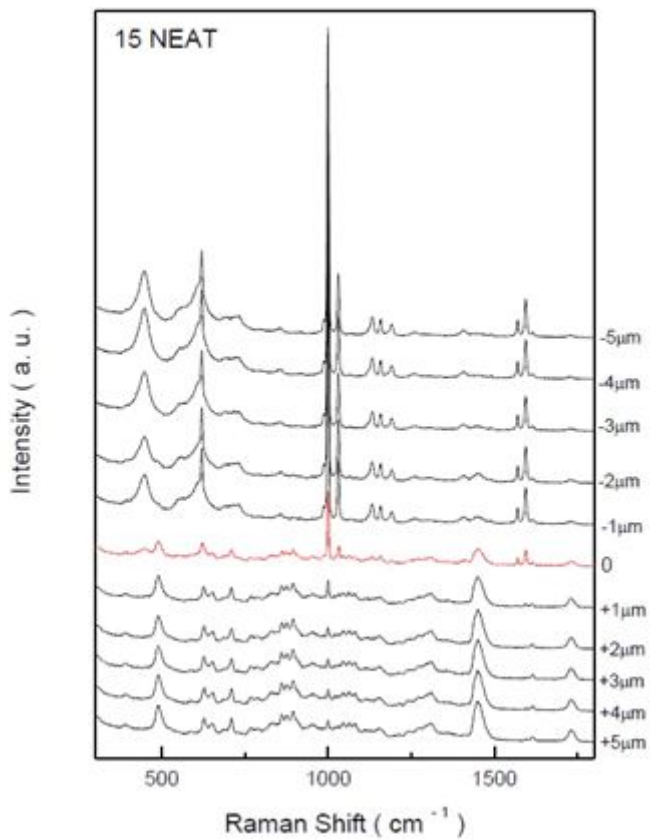


Figure 38. Depth profile of MAI-acrylic PSA on 1 day dwell time.

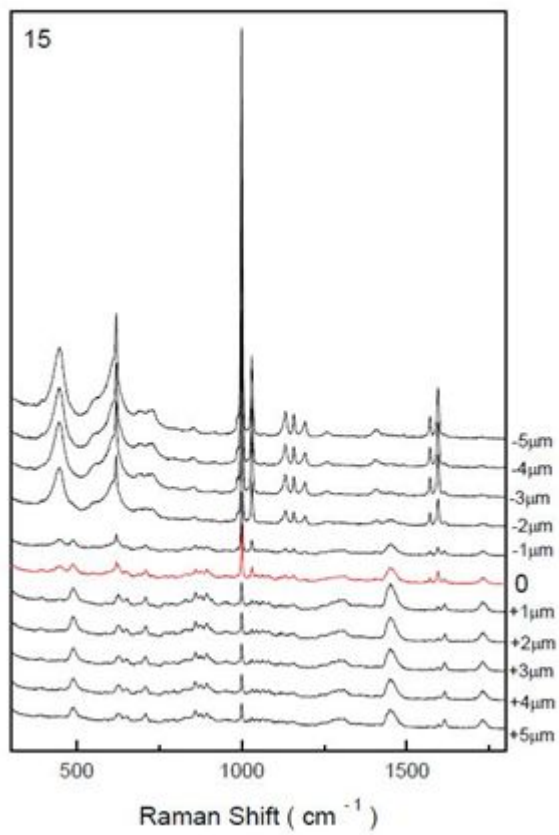


Figure 39. Depth profile of MAI-acrylic PSA on 15 day dwell time.

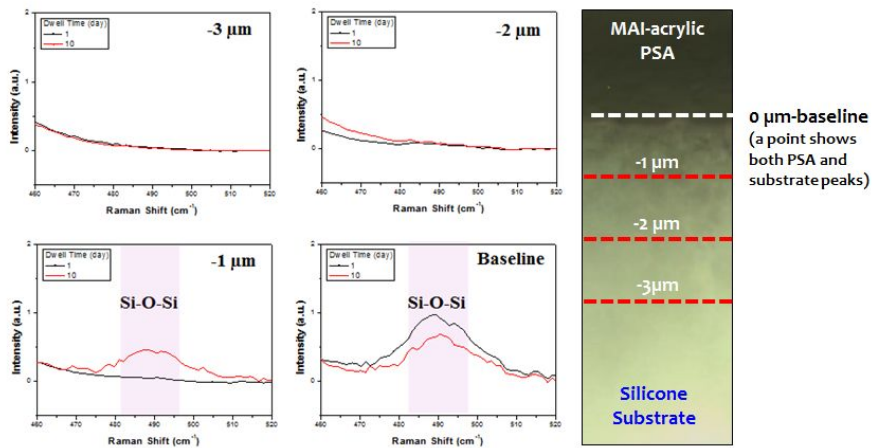


Figure 40. Raman spectra of MAI-acrylic PSA depending on relative distance from interfacial layer.

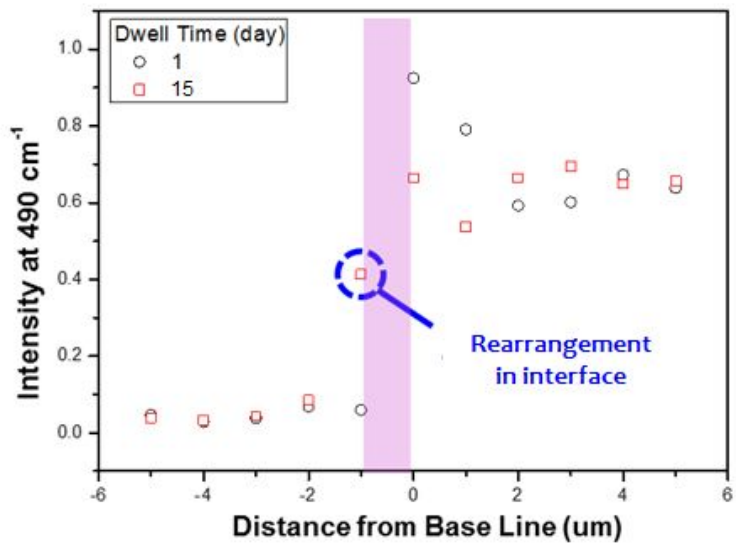


Figure 41. Depth profile between MAI-acrylic PSA and silicone substrate on Raman spectra at 490 cm⁻¹.

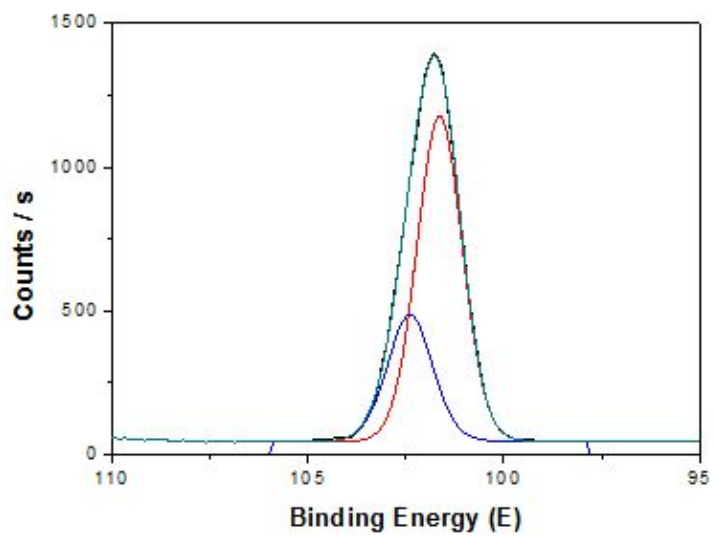


Figure 42. XPS results of MAI-acrylic PSA on 1 day dwell time.

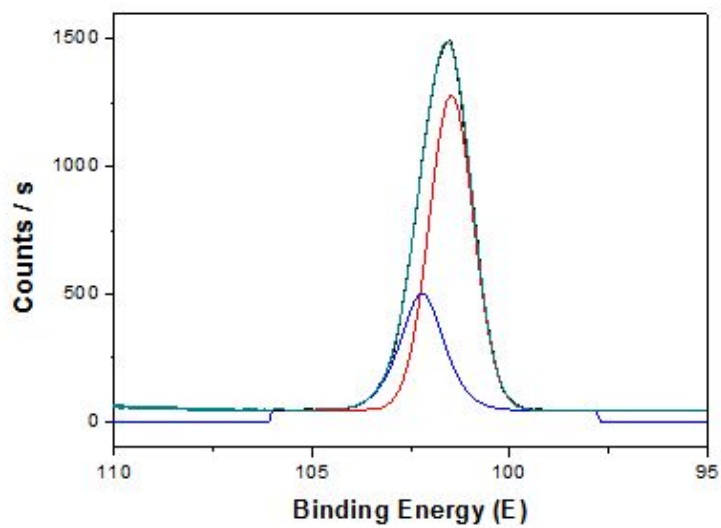


Figure 43. XPS results of MAI-acrylic PSA on 15 day dwell time.

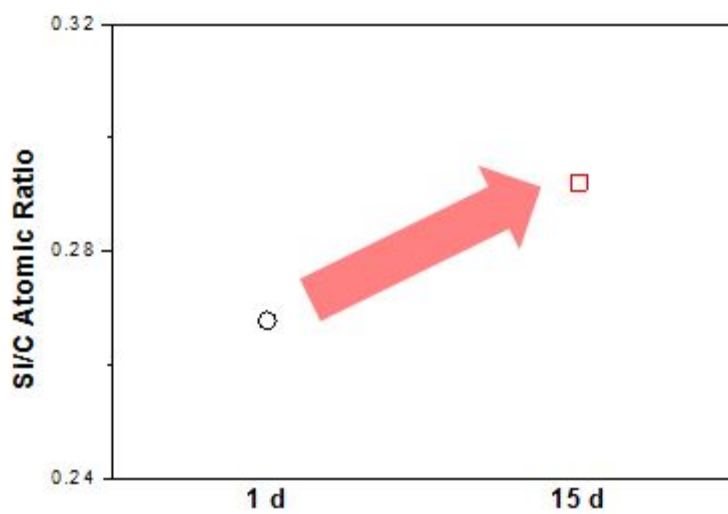


Figure 44. Si/Carbon atomic ratio of MAI-acrylic PSA depending on dwell time.

Table 8. Characteristics of some spectroscopic techniques suitable for studying polymeric materials (Long, *et al.*, 1977)

	XPS	IR and Raman	SIMS
Analysis environment	High vacuum	Ambient	UHV
Resolution	0.6eV	1 cm ⁻¹	0.1~1 amu
Elemental/molecular information	No H detection / chemical shifts	Functional group	All plus isotopes, MW, fragment
Detection limit	% of monolayer	% in volume	ppm/ppb elemental
Lateral resolution	5 mic	10 mic	10 nm
Depth sensitivity	>50Å	mic range	10Å
Sample damage	small, sometimes with unmonochromatized x-rays	none	High
Major outcomes	Elemental and chemical analysis, electronics structure	Molecular vibration, functional group	Low detection limits, molecular ions, fragmentation

Table 9. Contact angle photographs of MAI-acrylic PSA / LMW PSA.

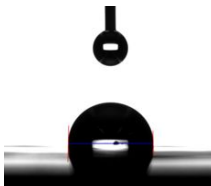
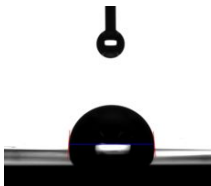
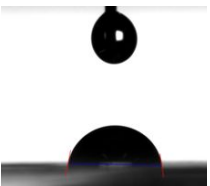
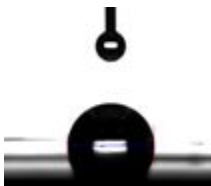
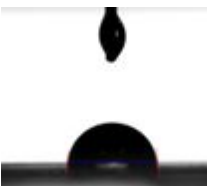
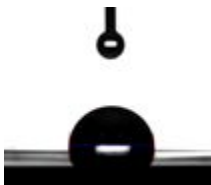
Sample name	D.I. water	Ethylene glycol	Diiodomethane
MAI20-LMW-0	 89.97	 83.04	 61.62
MAI20-LMW-10	 89.8	 81.49	 71.4
MAI20-LMW-20	 88.14	 82.78	 63.99
MAI20-LMW-50	 87.09	 80.79	 57.77

Table 10. Atomic ratio of MAI-acrylic surface depending on dwell time

Dwell time (day)	C1s (%)	O1s (%)	Si2p (%)
1	62.68	20.54	16.78
15	59.29	20.55	17.96

Chapter 4

Concluding Remarks

Synthesis and adhesion properties of MAI-acrylic PSAs with PDMS-based macro azoinitiator

MAI(macro-azo initiator) is possible to dissolve in organic solvents and easily can introduce the polydimethylsiloxane unit in the polymer chain. MAI initiator have a miscibility with organic solvent and monomers. Using solution polymerization, acrylic PSA with silicone structure can be polymerized effectively. Using FTIR and GPC, the polymerization process and polymerized PSA was monitored. The molecular weight of MAI-acrylic PSA shows decreasing depending on MAI content, PDI is increasing depending on MAI contents.

MAI-acrylic PSA shows a lower peel strength and probe tack with compared with acrylic PSA with AIBN, but SAFT or heat resistance is higher than acrylic PSA using AIBN. The appearance of coated film is a little hazy due to difference of refractive index between PDMS structure and acrylic structure.

Blending and adhesion properties of MAI-acrylate PSAs / Low Mw PSA / Polybutene(PB)

In previous chapter, the MAI-acrylic PSA was synthesized by radical polymerization. The peel strength and tack property is lower results than acrylic PSA using AIBN. To optimize adhesion properties such as peel strength and probe tack, low molecular wieght PSA (LMW) and polybutene were used in this study. The LMW of PSA has about 62,000 M_n . With blending by LMW PSA, peel strength and probe tack can be increased in range of 10~50 part. But on teflon, peel strength and probe tack cannot be

shown to advantage.

Polybutene (PB) is low molecular weight polymer with miscible with PSA. Using blending with PB, MAI-acrylic PSA shows higher peel strength and probe tack on SUS and Teflon. To bond onto low surface energy substrate, the low molecular polymer is needed to acquired fully bonding and fibrillation.

Adhesion properties and surface analysis of MAI-acrylate PSA / Low Mw PSA depending on dwell time

The MAI-LMW acrylic PSA has inhomogeneous structure with acrylic and PDMS molecules. On silicone substrate, the peel strength was evaluated depending on dwell time. As increasing MAI content, the MAI-LMW acrylic PSA shows higher peel strength depending on dwell time. And failure mode of peeling is changed from stick-slip to interfacial failure on time. We assume that interface between MAI-LMW acrylic PSA and silicone substrate was changed on dwell time to give increasing peel strength and change of failure mode.

For a better understanding influence of the inhomogeneities on the material properties, it is desirable to obtain information of the depth profile. To obtain directly the desired chemical and morphological information at high spatial resolution, infrared and Raman microscopy appear suitable techniques. Using microscope, the interface and depth point can be evaluated by Raman spectra. From Raman spectrum, the Si-O-Si bands moves from interface to silicone substrate after dwell time. Using XPS, chemical composition of surface during dwell time was evaluated. Si/Carbon % ratio is increasing depending

on dwell time. Therefore, MAI-LMW acrylic PSA can do rearrangement or migration into silicone substrate.

References

A. Diethert, K. Ecker, Y. Peykova, N. Willenbacher, P. Müller-Buschbaum (2011). Tailoring the near-surface composition profiles of pressure-sensitive adhesive films and the resulting mechanical properties. *ACS Appl. Mater. Interfaces* 3(6): 2012–2021.

A. Diethert, Y. Peykova, N. Willenbacher, P. Müller-Buschbaum (2010). Near-surface composition profiles and the adhesive properties of statistical copolymer films being model systems of pressure sensitive adhesive films. *ACS Appl. Mater. Interfaces* 2(7): 2060–2068.

A. Kinloch (2012). *Adhesion and adhesives: science and technology*. Springer Science & Business Media.

A. Kowalski, Z. Czech & Ł. Byczyn'ski (2013). How does the surface free energy influence the tack of acrylic pressure-sensitive adhesives (PSAs). *J. Coat. Technol. Res.* 10(6): 879–885.

A. Mata, A. J. Fleischman, S. Roy (2005). Characterization of polydimethylsiloxane (PDMS) properties for biomedical micro/nanosystems. *Biomedical Microdevices* 7(4): 281-293.

A. N. Gent, G. R. Hamed (1997) Peel mechanics of adhesive joints, *Polym.Eng.Sci.* 17: 462-466.

A. Zosel (1998). The effect of fibrillation on the tack of pressure sensitive adhesives. *Int. J. Adhes. Adhes.* 18: 265-271.

- B. D. Ratner, A. Chilkoti, D. G. Castner (1992) Contemporary methods for Characterizing Complex Biomaterial Surfaces. *Biologically Modified Polymeric Biomaterial Surfaces*. 28(3): 25-36.
- B. T. Hong, K. S. Shin, D. S. Kim (2005). Ultraviolet-curing behavior of an epoxy acrylate resin system. *Journal of Applied Polymer Science* 98(3): 1180-1185.
- D. A. Long (1977). *Raman spectroscopy*. New York.
- D. Briggs (1998). *Surface analysis of polymers by XPS and static SIMS*. Cambridge University Press.
- D. H. Lim, H. S. Do, H. J. Kim, J. S. Bang, G. H. Yoon (2002). Preparation of SIS/SBS-based UV-cross-linkable pressure-sensitive adhesives using the thiol-ene reaction. *Journal of Adhesion Science and Technology* 21(7): 589-603.
- D. J. Kim, H. J. Kim (2005). Effect of substrate and tackifier on peel strength of SIS (styrene-isoprene-styrene)-based HMPSAs. *International Journal of Adhesion and Adhesives* 25(4): 288-295.
- D. M. Brewis, D. Briggs (1981). Adhesion to polyethylene and polypropylene. *Polymer* 22(1): 7-16.
- D. Satas (2002). *Handbook of pressure sensitive adhesive technology and applications*. Satas & Associates, Warwick, Rhode Island.

- E. G. Shafrin, W. A. Zisman (1960). Constitutive relations in the wetting of low energy surfaces and the theory of the retraction method of preparing monolayers. *J. Phys. Chem.* 64(5): 519–524.
- E. P. Chang (1997). Viscoelastic properties of pressure-sensitive adhesives. *The Journal of Adhesion* 60(1-4): 233-248.
- F. Awajaa, M. Gilbertb, G. Kellya, B. Foxa, P. J. Pigramb (2009). Adhesion of polymers. *Progress in Polymer Science* 34(9): 948–968.
- G. Akoval, T. T. Torun, E. Bayramli, (1998). Mechanical properties and surface energies of low density polyethylene-poly(vinyl chloride) blends. *Polymer* 39(6-7): 1363-1368.
- G. Pan, L. Wu, Z. Zhang, D. Li (2001). Synthesis and characterization of epoxy-acrylate composite latex. *Journal of Applied Polymer Science* 83(8): 1736–1743.
- H. Gleskova, S. Wagner, D. S. Shen (1995). Electrophotographic patterning of thin-film silicon on glass foil. *IEEE Elec. Dev. Lett.* 16: 418-420.
- H. Gleskova, S. Wagner, W. Soboyejo, Z. Suo (2002). 14 - Formation of electrical circuits in textile structures. *J. Appl. Phys.* 92: 6224-6229.
- H. Gleskova, S. Wagner, Z. Suo (1998). Photoresist-free fabrication process for a-Si:H thin film transistors. *Journal of Non-Crystalline Solids* 227-230: 1217-1220.

H. Gleskova, S. Wagner, Z. Suo (1999). Delocalizing strain in a thin metal film on a polymer substrate. *Original. Appl. Phys. Lett.* 75: 3011-3013.

H. S Tan, W. R Pfister (1999). Pressure-sensitive adhesives for transdermal drug delivery systems. *Pharmaceutical Science & Technology Today* 2(2): 60–69.

H. S. Do, S. E. Kim, H. J. Kim (2003) *Adhesion—current research and applications*. Wiley-VCH.

H. S. Joo, H. S. Do, Y. J., Park, H. J. Kim (2006). Adhesion performance of UV-cured semi-IPN structure acrylic pressure sensitive adhesives. *Journal of Adhesion Science and Technology* 20(14): 1573-1594.

H. S. Joo, Y. J. Park, H. S. Do, H. J. Kim (2007). The curing performance of UV-curable semi-interpenetrating polymer network structured acrylic pressure-sensitive adhesives. *Journal of Adhesion Science and Technology* 21(7): 575-588.

J. Asahara, N, Hori, A. Takemura, H. Ono (2003). Crosslinked acrylic pressure-sensitive adhesives. I. Effect of the crosslinking reaction on the peel strength. *Journal of Applied Polymer Science* 87(9): 1493-1499.

J. Asahara, A. Takemuraa, N. Horia, H. Onoa, H. Matsuib (2004). Crosslinked acrylic pressure sensitive adhesives. 3. Effect of adherend on film formation. *Polymer* 45(14): 4917–4924.

J. Kajtnaa, B. Likozarb, J. Golobb, M. Krajnc (2008). The influence of the polymerization on properties of an ethylacrylate/2-ethyl hexylacrylate pressure-sensitive adhesive suspension. *International Journal of Adhesion and Adhesives* 28(7): 382–390.

J. L. Koenig (1999). *Spectroscopy of polymers*. Elsevier.

K. S. Anseth, L. M. Kline, T. A. Walker, K. J. Anderson, C. N. Bowman (1996). Reaction kinetics and volume relaxation during polymerizations of multiethylene glycol dimethacrylates. *Macromolecules* 28: 2491-2499.

J. M. Zajackowski (2010). *Pressure sensitive adhesives in high performance applications*. The Adhesive and Sealant Council.

K. Moussa, C. Decker (1993). Semi interpenetrating polymer networks synthesis by photocrosslinking of acrylic monomers in a polymer matrix. *Journal of Polymer Science Part A: Polymer Chemistry* 31(10): 2633-2642.

L. L. Christopher, L. B. William (2006) Acrylic pressure sensitive adhesives having controlled placement of functional groups. PSTC TECH 32 Technical Seminar.

M. Fujita, A. Takemura, H. Ono, M. Kajiyama, S. Hayashi, H. Mizumachi (2000). Effects of miscibility and viscoelasticity on shear creep resistance of natural-rubber-based pressure-sensitive adhesives. *Journal of Applied Polymer Science* 75(12): 1535–1545.

M. Schneemilch, R. A. Hayes, J. G. Petrov, J. Ralston (1998). Dynamic wetting and dewetting of a low-energy surface by pure liquids. *Langmuir* 14(24): 7047–7051.

M. X. Xu, W. G. Liu, J. Wang, W. Gao, K. D. Yao (1997). Surface rearrangement of vinyl acetate and acrylate terpolymer adhesives investigated by dynamic contact angles. *Polymer International* 44(4): 421–427.

M. Manea, J.M. Asua, J. L. Keddie (2003). Waterborne, nanocomposite pressure-sensitive adhesives with high tack energy, optical transparency, and electrical conductivity. *Advanced Material* 18: 2730–2734.

R. L. McCreery (2005). *Raman spectroscopy for chemical analysis*. John Wiley & Sons.

R. Muppalla, S. K. Jewrajka (2012). Synthesis morphology and properties of poly(dimethylsiloxane)/poly(n-butyl acrylate) mixed soft block-based copolymers: A new class of thermoplastic elastomer. *Polymer* 53(7): 1453–1464.

S. Hayashi, H. J. Kim, M. Kajiyama, H. Ono, H. Mizumachi, Z. Zufu (1999). Miscibility and pressure-sensitive adhesive performances of acrylic copolymer and hydrogenated rosin systems. *J. Appl. Polym. Sci.* 71: 651-663.

- S. Sun , M. Li, A. Liu (2013). A review on mechanical properties of pressure sensitive adhesives. *International Journal of Adhesion and Adhesives* 41: 98–106.
- S. Wagner, H. Gleskova, I. Cheng, J. C. Sturm (2007). *Flexible flat panel displays*. Wiley.
- S. Y. Lin, C. J. Lee, Y. Y. Lin (1991). The effect of plasticizers on compatibility, mechanical properties, and adhesion strength of drug-free Eudragit E films. *Pharm. Res.* 8: 1137-1143.
- T. Hata, J. Kumanotani (1994). Viscoelastic properties of epoxy resin. I. Effect of prepolymer structure on viscoelastic properties. *Journal of Applied Polymer Science* 15(10): 2371-2380.
- T. Igarashi (1975). Mechanics of peeling of rubbery materials. *J. Polym. Sci. Polym. Phys. Ed.* 13: 2129-2134.
- T. Ryhanen, M. A. Uusitalo, A Karkkainen (2010). *Nanotechnologies for future mobile devices*. Cambridge.
- T. Sekitani, H. Nakajima, H. Maeda, T. Fukushima, T. Aida, K. Hata, T. Someya (2009). Stretchable active-matrix organic light-emitting diode display using printable elastic conductors. *Nature Materials* 8: 494–499.

T. Sekitani, T. Someya (2011). Stretchable and foldable displays using organic transistors with high mechanical stability. *SID Symposium Digest of Technical Papers* 42(1): 276–279.

W. Jiang, J. He, F. Xiao, S. Yuan, H. Lu, B. Liang (2015). Preparation and antiscaling application of superhydrophobic anodized CuO nanowire surfaces. *Ind. Eng. Chem. Res.* 54(27): 6874–6883.

W. S. Wong, A. Salleo (2009). *Flexible electronics: materials and applications*. Springer.

X Sun, J Liu, M. L. Lee (2005). Surface-reactive acrylic copolymer for fabrication of microfluidic devices. *Anal. Chem.* 77(19): 6280–6287.

X. Zhang, F. Shi, J. Niu, Y. Jiang, Z. Wang (2008). Superhydrophobic surfaces: from structural control to functional application. *J. Mater. Chem.* 18: 621-633.

Y. Iyengar, D. E. Ericson (1967). Role of adhesive-substrate compatibility in adhesion. *Journal of Applied Polymer Science* 11: 2311-2324.

Z. Czech (2007). Synthesis and cross-linking of acrylic PSA systems. *Journal of Adhesion Science and Technology* 21(7): 625-635.

Z. Czech, M. Urbala, D. Martysz (2004). Investigation of the tensile properties of epoxy resin-monomer systems using cationic UV-crosslinkable blends. *Polymers for Advanced Technologies* 15(7): 387~392.

Z. Czech, M. Wojciechowicz (2006). The crosslinking reaction of acrylic PSA using chelate metal acetylacetonates. *European Polymer Journal* 42(9): 2153-2160.

Z. Czech, R. Pelech (2009). The thermal degradation of acrylic pressure-sensitive adhesives based on butyl acrylate and acrylic acid. *Progress in Organic Coatings* 65(1): 84-87.

Z.Czech, R. Milker (2005). Development trends in pressure-sensitive adhesive systems. *Materials Science-Poland* 23(4): 1015~1022.

Zhuang, H., Gardella J. A. (1996). Spectroscopic characterization of polymer surfaces. *MRS Bulletin* 21(01): 43-48.

초록

Abstract

저표면 에너지 기재 접착용 실리콘-아크릴레이트 점착제의 합성 및 물성

임동혁

서울대학교 농업생명과학대학
산림과학부 환경재료과학 전공

최근 IT 업계는 사물인터넷, 사회적 IT 융합을 목적으로 스마트 폰, 스마트 밴드, 웨어러블 디바이스, 모바일과 금융 서비스의 융합 등의 비약적인 발전을 보이고 있다. 이를 위해서 스마트 디바이스는 보다 작아지고, 얇아지고 저렴해짐을 요구하고 있다.

미래의 스마트 디바이스는 유연성, 슬림성, 컴팩트성을 가지고 있어야 하며 이를 위한 기재로는 실리콘 재질의 탄성체를 검토하고 있다. 실리콘 탄성체는 내열성, 유연성, 내충격성, 내환성성을 가지고 있지만 낮은 표면 에너지와 소프트한 표면을 가지고 있어서 물리적 화학적 결합이 어려운 단점을 가지고 있다.

일반적으로 실리콘 탄성체는 표면장력이 낮은 실리콘 및 불소계의 접착제 및 점착제를 사용하고 있지만 고가의 불소이형필름 및 실리콘 소재의 사용으로 그 사용이 제한적이다.

본 연구에서는 낮은 표면장력을 가지는 PDMS계 열 개시제(MAI)를 이용하여 변성 아크릴 점착제를 합성하였다. MAI는 PDMS 블록과 열 개시가 가능한 아조(azo)그룹을 가지고 있어서 일반적인 아크릴 점착제 합성과 동일한 과정으로 실리콘이 도입된 아크릴 점착제 제조가 가능하다. 이렇게 제조된 MAI-아크릴 점착제의 점착물성을 제어하기 위해서 저분자량의 아크릴 점착제를 별도로 제조하여 블렌딩을 하여 점착물성의 변화를 살펴보았다. 가소제의 역할을 하는 폴리부텐을 분자량별로 블렌딩하여 점착물성의 변화를 살펴보고 표면장력이 낮은 다양한 기재에 대한 점착력이 올라감을 확인하였다.

실리콘 기재에 부착력을 점착시간에 따라서 살펴보고, 파괴거동을 살펴본 결과 시간에 따라서 표면의 화학적 변화가 예상되었으며, 이를 contact angle, Raman spectroscopy, XPS를 이용하여 표면분석을 시행하고 표면의 변화를 관찰하였다.

이러한 연구는 난점착 표면에 접착이 가능한 실리콘-아크릴 점착제를 간편히 제조하고 이의 접착기작을 밝힘으로써 추후 플렉시블 디바이스의 접착 과정에 도움을 줄 수 있을 것이다.

Keywords: pressure sensitive adhesive, low surface energy pressure sensitive adhesives, modified acrylic PSA, adhesion performance

Student Number : 2005-30361